

# Physics from the lattice: glueballs in QCD; topology; $SU(N)$ for all $N$ .

Michael J Teper\*  
*Department of Physics*  
*University of Oxford*  
*Oxford, OX1 3NP, U.K.*

arXiv:hep-lat/9711011v1 6 Nov 1997

hep-lat/9711011

---

\*Lectures at the Isaac Newton Institute NATO-ASI School, June 1997

# 1 Introduction

In these lectures I will show, through three examples, how current lattice calculations are able to tell us interesting things about the continuum physics of non-Abelian gauge theories.

My first topic concerns the glueball spectrum. The physics question here is: where, in the experimentally determined hadron spectrum, are the glueballs hiding? I will first summarise what lattice calculations tell us about the continuum glueball spectrum of the  $SU(3)$  gauge theory. I will then discuss what this tells us about the masses of the corresponding ‘bare’ glueballs in QCD. I will then turn to the experimental spectrum with some discussion of the interpretation of the observed states in the quark model. Finally I will pinpoint the experimental states most likely to have large glueball components.

The second topic concerns topological fluctuations in the  $SU(3)$  gauge theory. Here the simplest physics question is: are these fluctuations large enough to be consistent with the observed large  $\eta'$  mass? Thanks to Witten and Veneziano this is a question that can be posed in the pure gauge theory. We shall see that the fluctuations of the topological charge do indeed have the required magnitude. Along the way I will discuss the problems with topology on a lattice. I then move onto the much less straightforward question concerning the structure of these vacuum fluctuations: e.g. what is the size distribution of instantons? I will discuss some preliminary calculations that show the mean size to be about  $\bar{\rho} \sim 0.5 fm$ . I will also point to some intriguing evidence for a long distance polarisation of the topological fluctuations.

My third topic concerns the physics of  $SU(N_c)$  gauge theories as a function of the number of colours,  $N_c$ . This will be mainly in 2+1 dimensions, since that is where we have good calculations. I will describe calculations of the mass spectrum for  $N_c \leq 4$  which explicitly show that for  $N_c \geq 2$  mass ratios are independent of  $N_c$  up to a modest  $\sim 1/N_c^2$  correction. This is a very elegant result: it tells us that all the apparently different  $SU(N_c)$  theories are actually one single theory,  $SU(\infty)$ , to a reasonable first approximation. There is some very preliminary evidence, as I will show, that the same is true for  $D = 3 + 1$ .

## 2 Glueballs in QCD

Ideally I should be telling you what happens when you simulate QCD with realistically light quarks. But it is going to be a few years yet before I can do that. What current lattice Monte Carlo calculations are able to provide is predictions for the low-lying mass spectrum of the continuum  $SU(3)$  gauge theory without quarks. These states are glueballs - there being nothing other than gluons in the theory. If you want hadrons with quarks then you can propagate quarks in this gluonic vacuum and then tie such propagators together so that the object propagating has the appropriate hadronic quantum numbers. That is to say, you calculate hadron masses in the relativistic valence quark approximation. (This is usually referred to as the ‘quenched approximation’ to QCD.) The spectrum one obtains this way is a remarkably good approximation to the observed hadron spectrum. This is not too

surprising: one reason we were able to learn of the existence of quarks in the first place is because the low-lying hadrons are in fact well described by a simple valence quark picture.

Suppose that we begin with our  $SU(3)$  gauge theory and then couple to it 3 flavours of very heavy quarks. Initially the spectrum will contain the usual light glueball spectrum, supplemented by a spectrum of very heavy quarkonia that can be well accounted for in terms of a valence quark potential model. Let us now gradually reduce the quark masses towards their physical values. In principle the glueball and quarkonia states might entirely change their character once their masses become comparable. However, as we remarked above, the experimental light quark spectrum still seems to retain the essential features of valence quark physics. If the quarkonia are not qualitatively altered, it seems reasonable to think that neither will the glueballs be. Of course if a quarkonium state and a glueball are close enough in mass they will mix. However there is reason to believe that this mixing is weak. The reason is the Zweig (OZI) rule: hadron decays where the initial quarks all have to annihilate are strongly suppressed. The classic example is the  $\phi$  meson. Such a decay may be thought of as  $quarks \rightarrow glue \rightarrow quarks$ . Glueball mixing with quarks should therefore be  $\sqrt{OZI}$  suppressed. As should glueball decays into hadrons composed of quarks. The existence of such a suppression is supported by a recent lattice calculation [1].

The picture we have in mind is therefore as follows. The glueballs will only be mildly affected by the presence of light quarks. They will decay into, say, pions but their decay width will be relatively small; and there will be a correspondingly small mass shift. Only if there happens to be a flavour singlet quarkonium state close by in mass will things be very different, because of the mixing of these nearly degenerate states. In this context we expect ‘close by’ to mean within  $\sim 100 MeV$ . So we view the glueballs in the pure  $SU(3)$  gauge theory as being the ‘bare’ glueballs of QCD which may mix with nearby quarkonia to produce the hadrons that are observed in experiments. All this is an assumption of course, albeit a reasonable one. If true it tells us that the glueballs, whether mixed with quarkonia or not, should lie close to the masses they have in the gauge theory. So we now turn to the calculation of those masses.

I shall begin by reviewing the available lattice calculations, placing a particular emphasis on exposing the sources of systematic error in arriving at a final mass prediction in  $MeV$  units. I do this in some detail, so that you are able to judge for yourselves the credibility of lattice mass estimates.

As we shall soon see, it is only for three states that the lattice calculations are reliable enough that we can extract continuum predictions: the lightest scalar,  $0^{++}$ , tensor,  $2^{++}$ , and pseudoscalar,  $0^{-+}$ , glueballs. For other states we do have calculations for one or two values of the lattice spacing  $a$ , but that is not enough to extrapolate to  $a = 0$ . Nonetheless the lattice results strongly suggest that glueballs with other  $J^{PC}$  are heavier [2].

The lightest glueball is the  $0^{++}$ , and it is for this state that we have the most accurate lattice predictions. Although there have been recent estimates for the mass that appear to differ, e.g.  $1.55 \pm 0.05 GeV$  [2] and  $1.74 \pm 0.07 GeV$  [3, 1], we shall see that this difference is illusory. In fact the apparent difference reflects different ways of extrapolating to the continuum limit and different ways of introducing physical  $MeV$  units into the pure gauge theory. That is to say, it reflects particular systematic errors which we need to estimate and

this we try to do. Since we find that the various lattice calculations are consistent, we are able to carry out a global analysis that provides the best available glueball mass estimate. We find  $m_{0^{++}} = 1606 \pm 73 \pm 130 MeV$  where the first error is statistical and the second is systematic. Performing a similar analysis for the lightest tensor and pseudoscalar glueballs we find  $m_{2^{++}} = 2200 \pm 73 \pm 130 MeV$  and  $m_{0^{-+}} = 2100 \pm 73 \pm 130 MeV$ .

From the experimental and phenomenological point of view the scalar sector is complex, and I will review the current state of play. As we shall see, there appear to be too many scalar states to be explained as quarkonia, and the strongest candidates for states with large gluonic components are the  $f_0(1500)$  and the  $f_{(J=0?)}(1710)$ . This possibility is strongly reinforced by the fact that these are the only experimental states that are compatible with the lattice mass estimate in the previous paragraph.

In order to assess which states have the largest gluonic components, it is important to understand the mixing between nearby quarkonia and glueballs. I shall briefly discuss what happens in the case of mixing between a glueball and the lightest singlet and octet scalar quarkonium multiplets.

For this review I have drawn very heavily on [4].

## 2.1 Calculating glueball masses

I begin by briefly reminding you of some general aspects of lattice calculations. (For more detail see the lectures by Chris Michael at this School and the books by Creutz [5] and Montvay and Munster [6].) In a lattice calculation (Euclidean) space-time is discretised, usually onto a hypercubic lattice. What we calculate is the mass spectrum of the discretised theory, but what we actually want is the corresponding spectrum of the continuum theory. Because the theory is renormalisable, the effects of the lattice spacing,  $a$ , on physical length scales will vanish as  $a \rightarrow 0$ . Since QCD has effectively one length scale,  $\sim 1 fm$ , one expects the effects of the discretisation to become negligible once  $a \ll 1 fm$ . The same is true of the gauge theory without quarks. (By ‘ $1 fm$ ’ I really mean some characteristic physical length scale. How one introduces actual fermi units into the pure gauge theory is something we shall return to below.) The lattice spacing is varied by changing the value of the bare (inverse) coupling which appears in the lattice action:  $\beta = 6/g^2$ . Since the theory is asymptotically free, we know that in order to approach the continuum limit,  $a \rightarrow 0$ , we need to take  $g^2 \rightarrow 0$  and so  $\beta \rightarrow \infty$ . Indeed for sufficiently small  $g^2$  one can determine the relationship between  $a$  and  $g^2$  in low-order perturbation theory. (Although in practice the latter does not work well for the range of couplings currently accessible.) Reducing  $a$  makes the calculation numerically more intensive for various reasons. An obvious one is that if we wish to maintain a constant volume, the number of lattice sites grows  $\propto 1/a^4$ . It is only in recent years that calculations for very small values of  $a$  have become practical. As we shall see, the mass calculations I shall use here have been performed over a range of lattice spacings  $0.18 fm \geq a \geq 0.06 fm$ , corresponding to couplings  $5.7 \leq \beta \leq 6.4$ .

We now outline the main steps in a lattice Monte Carlo calculation of a glueball mass with a view to exposing the main different sources of systematic error. (So we ignore various

unilluminating technicalities and skate over various qualifications that are irrelevant for this purpose.)

- *Extracting lattice masses.* The first step is to calculate the glueball spectrum on a lattice, for a given space-time volume  $V$  and for a particular lattice spacing  $a$ . The Euclidean time translation operator is  $e^{-Ht}$ , where  $H$  is the Hamiltonian of the theory. Thus the correlation function of an operator with some particular  $J^{PC}$  quantum numbers will, for large enough values of  $t$ , vary as  $e^{-m_0 t}$  where  $m_0$  is the lightest mass with those quantum numbers. We calculate such propagators numerically for  $t$  large enough that we see this asymptotic exponential decay. From the exponent we extract the mass. Since  $t$  is given in lattice units ( $t = an$  where  $n$  is the number of lattice spacings) the exponent is  $m_0 t = m_0 a n$  and so what we actually obtain is the mass in lattice units, i.e.  $am_0$ . The statistical errors are straightforward to estimate. However there is also a systematic error that has to do with determining the range of  $t$  where the asymptotic exponential dominates. We do not attempt to quantify this error but simply note that it will become increasingly important for the heavier glueball states (such as the tensor and pseudoscalar) where the exponential decrease with  $t$  of the ‘signal’, and hence its immersion into the statistical noise, is more rapid.

- *Finite  $V$  corrections.* The second step is to determine the corrections due to the fact that the volume is finite. For most quantities the functional forms of the leading large- $V$  corrections are known theoretically; typically they will be of the form  $\delta m \propto \exp\{-camL\}$  where  $am$  and  $L$  are the mass-gap and lattice size in lattice units [7]. By doing calculations for a variety of volumes at some chosen value of  $a$ , any unknown constants in these expressions can be fitted and the resulting formulae can be used to apply corrections at other values of  $a$ . Since the calculations we use here have been performed on periodic volumes of typical sizes 1.5 to 2.0 fm, these corrections are smaller than our typical statistical errors; but it is hard to determine them more accurately than that. This provides another source of systematic error.

- *Finite  $a$  corrections.* The calculated glueball mass will depend on  $a$ ; and it will do so in two ways. Firstly, it is obtained in lattice units,  $am$ . This trivial dependence is removed when we take the ratio of two masses:  $am_1/am_2 \equiv m_1/m_2$ . The non-trivial  $a$  dependence is due to the distortion of the dynamics by the discretisation. For the lattice action we use and for quantities such as glueball mass ratios it is known that the leading small- $a$  correction is  $O(a^2)$  [8]. So for small enough  $a$  we can extrapolate our calculated mass ratios to  $a = 0$  using

$$\frac{m_1(a)}{m_2(a)} = \frac{m_1(a=0)}{m_2(a=0)} + c(am)^2 \quad (1)$$

where  $m$  may be chosen to be  $m_1$  or  $m_2$  or some other physical mass: the difference between these choices is clearly higher order in  $a^2$ . Such neglected higher order terms in the extrapolation are another source of systematic error.

- *Introducing the MeV scale.* Having obtained the continuum mass spectrum in the form of mass ratios, we want to express the masses in usual  $MeV$  units. This can be done if at least one of the masses corresponds to a quantity whose value is known in  $MeV$ . For example the potential between heavy quarks is linear for large separations:  $V(r) \simeq \sigma r$  where  $\sigma$  is called the string tension. In simple string pictures for high  $J$  hadrons  $\sigma$  is related to the

slope,  $\alpha'$ , of Regge trajectories by  $\alpha' = 1/2\pi\sigma$  and this provides the conventional estimate  $\sqrt{\sigma} \simeq 400 - 450 \text{ MeV}$  [9]. Knowing the continuum value of  $m_G/\sqrt{\sigma}$  we can now express  $m_G$  in  $\text{MeV}$  units. Of course one may distrust this particular argument for the value of  $\sigma$ . An alternative is to calculate quark propagators in the pure gauge theory and from these to form hadron propagators. From the asymptotic exponential decay of the latter we obtain quarkonium masses in the (relativistic) valence quark approximation. For example, we can obtain the continuum limit of the mass ratio  $m_\rho/\sqrt{\sigma}$ . Setting  $m_\rho = 770 \text{ MeV}$  we obtain a value for  $\sqrt{\sigma}$  and hence for the glueball mass  $m_G$ . Or we might set the scale using the  $\phi$ -meson or the nucleon instead of the  $\rho$ . While the mass spectrum one obtains in the quenched approximation is remarkably close to that which is experimentally observed, it is not exactly the same and so these different ways of setting the physical scale will lead to slightly different glueball masses. This is a source of systematic error.

The first three types of systematic error can be made arbitrarily small by sufficiently improving the numerical calculations (in obvious ways). The error in setting the  $\text{MeV}$  scale is qualitatively different. It is intrinsic to working within the quenched approximation. How do we estimate it? There are some quantities which we know are going to be sensitive to the absence of vacuum  $q\bar{q}$  fluctuations, e.g. the  $\eta'$  mass or the topological susceptibility. These should obviously not be used to set the  $\text{MeV}$  scale in the pure gauge theory. There are other quantities which we expect to be no more sensitive to the absence of vacuum  $q\bar{q}$  fluctuations than the glueball masses themselves and which are therefore suitable quantities with which to attempt to set the  $\text{MeV}$  scale. These include the masses of typical quarkonia such as the  $\rho$  meson, the  $\phi$  meson, the nucleon, certain matrix elements, etc. Of course the ratios of these quantities cannot be exactly the same in full and quenched QCD and so the scale we extract will vary according to which of these quantities we choose to use. The extent of this variation can be used as an estimate of the systematic error.

## 2.2 The lightest glueballs

The values of the glueball masses that we shall use are from [11, 10, 2, 3] and those of the string tension are taken from [10, 2, 12]. As we have mentioned already, only the  $0^{++}$ ,  $2^{++}$  and  $0^{-+}$  glueballs are determined accurately enough that a continuum extrapolation is possible. In [2] you can find mass estimates for glueballs of widely varying  $J^{PC}$ , obtained for a very small lattice spacing. These do suggest that the three masses we shall obtain are in fact the lightest ones. There is clearly an urgent need for a new generation of lattice glueball calculations which will provide information on a much larger part of the continuum mass spectrum. For a preview of what these are likely to look like, see [13].

The first step is to take ratios of masses so that the scale,  $a$ , in which they are expressed cancels. We choose to take ratios of the glueball masses,  $am_G$ , to  $a\sqrt{\sigma}$  since this latter quantity has been very accurately calculated. Now we remarked above that for small enough  $a$  the leading discretisation effects in such mass ratios are  $0(a^2)$ . So for small enough  $a$  we expect

$$\frac{m_G(a)}{\sqrt{\sigma(a)}} = \frac{m_G(a=0)}{\sqrt{\sigma(a=0)}} + ca^2\sigma \quad (2)$$

We take all the available mass values and try to fit them using eqn 2. If a good fit is not possible we assume that this is because the largest values of  $a$  used is too large for the  $O(a^2)$  correction to be adequate. So we drop the mass corresponding to the largest value of  $a$  and try again. We keep doing this until we get a good fit. We find that the  $0^{++}$  glueball can be well fitted in this way over a range of lattice spacings  $0.18fm \geq a \geq 0.06fm$ , corresponding to couplings  $5.7 \leq \beta \leq 6.4$ . (Note that where we employ fermi units, these have been introduced using  $\sqrt{\sigma} = 440MeV$ ; a value that will be made plausible later on.) Such lattice spacings are small enough that we are not surprised that higher order terms in  $a^2$  should be small. We show the mass ratios in Fig 1 together with the best fit of the form in eqn 2. We obtain the *continuum* mass ratio:

$$\frac{m_{0^{++}}}{\sqrt{\sigma}} = 3.65 \pm 0.11 \quad (3)$$

The fit is obviously a very good one (with a confidence level of 85%) and it is clear that the calculations of the different groups are entirely consistent with each other.

In Fig 2 and Fig 3 I show corresponding plots for the  $2^{++}$  and  $0^{-+}$  glueballs. The former is well determined, and we obtain the continuum ratio

$$\frac{m_{2^{++}}}{\sqrt{\sigma}} = 5.15 \pm 0.21. \quad (4)$$

It is however clear that our control over the  $0^{-+}$  is marginal. This translates into a very large error when we perform the continuum extrapolation:

$$\frac{m_{0^{-+}}}{\sqrt{\sigma}} = 4.97 \pm 0.58. \quad (5)$$

We now wish to transform the above continuum glueball masses to physical  $MeV$  units. There are several reasonable ways to do this and how they differ will give us an estimate of the systematic error intrinsic to introducing physical units into a theory that is not quite physical.

As we remarked earlier, one way is to infer from the observed Regge slopes that  $\sqrt{\sigma} \simeq 400 - 450MeV$ . This estimate does however suffer from being somewhat model dependent. An alternative is to take lattice calculations of the mass of the  $\rho$  and extrapolate the ratio  $m_\rho/\sqrt{\sigma}$  to the continuum limit, just as we did for the glueball. The only difference with eqn 2 is that the leading correction will be  $O(a)$  rather than  $O(a^2)$ . We do this for two recent ‘state-of-the-art’ calculations: the GF11 collaboration [14] and the UKQCD collaboration [15] who use quite different discretisations for the quark action. UKQCD uses an improved action which should have smaller discretisation errors. We plot the two sets of ratios in Fig 4 with their corresponding continuum extrapolations. These give us

$$\frac{m_\rho}{\sqrt{\sigma}} = 1.72 \pm 0.08 \quad GF11 \quad (6)$$

and

$$\frac{m_\rho}{\sqrt{\sigma}} = 1.78 \pm 0.08 \quad UKQCD \quad (7)$$

respectively. It is reassuring that these two calculations are entirely consistent in the continuum limit, despite the fact that they have very different lattice discretisation corrections. (Indeed one can argue that the dominant correction in the UKQCD calculation will be  $0(a^2)$  rather than  $0(a)$ .) To extract a value for  $\sigma$  in  $MeV$  units we average the above results, set  $m_\rho = 770MeV$  and so obtain  $\sqrt{\sigma} = 440 \pm 15 MeV$ . We observe that this is entirely consistent with the scale we inferred from Regge slopes; but the argument is much cleaner here.

The error on  $\sigma$  is largely statistical. We now need to estimate the systematic errors as well. These are discussed in detail in [4]. There we consider errors due to finite volume corrections, to extrapolations in the quark mass, to uncertainties in our estimates of the lattice values of  $\sigma$  and to using the  $K^*$  or nucleon to set the scale rather than the  $\rho$ . We estimate a  $\pm 8\%$  systematic error in total. This leads to our final estimate for the value of the string tension as being:

$$\sqrt{\sigma} = 440 \pm 15 \pm 35 MeV \quad (8)$$

where the first error is statistical and the second is systematic.

We can now use this value in eqns 3- 5 to express our glueball masses in  $MeV$  units. We obtain

$$m_{0^{++}} = 1.61 \pm 0.07 \pm 0.13 GeV \quad (9)$$

$$m_{2^{++}} = 2.26 \pm 0.12 \pm 0.18 GeV \quad (10)$$

and

$$m_{0^{-+}} = 2.19 \pm 0.26 \pm 0.18 GeV. \quad (11)$$

The first error combines the statistical errors on the glueball and  $\rho$  continuum extrapolations, and the second is our estimate of the systematic error. This, then, is our best lattice prediction for the lightest glueballs prior to any mixing with nearby quarkonium states.

Where are the quarkonia? We are interested in flavour-singlet states because those are the ones that can mix with glueballs. It would clearly be very useful if lattice calculations were to provide estimates for the masses of the  $u\bar{u} + d\bar{d}$  and  $s\bar{s}$  mesons prior to their mixing with glue. One could then introduce the mixing with the scalar glueball using the (standard) formalism described below and compare the resulting states with the experimental spectrum. There are some indications from recent lattice calculations [16, 17] that there is a scalar  $s\bar{s}$  state close to the scalar glueball mass. However these quenched calculations do not try to incorporate the essential quark annihilation contributions and so must be regarded as indicative at best. We will therefore turn now to experiment and phenomenology.

## 2.3 Experiment and phenomenology

An illuminating (if arbitrary) starting point is provided by first considering the lightest  $2^{++}$  mesons. In the quark model [18] these are very similar to the scalars: the quark spins are aligned in both cases and the only difference is that the net spin is parallel to the unit orbital angular momentum for the tensors and antiparallel for the scalars - which, in quark potential models, leads to minor differences in the masses [19]. However in the real world we expect the tensors to have narrower decay widths than the scalars because their decays into



light pseudoscalars require non-zero angular momentum and corresponding near-threshold suppression factors. Thus they should be easier to identify experimentally - and that is their interest for us here.

Experimentally we find the following lightest tensor states [20]. There is an isoscalar  $f_2(1270)$  with width,  $\Gamma \sim 185 MeV$ , a second isoscalar  $f_2'(1525)$  ( $\Gamma \sim 76 MeV$ ), an isovector  $a_2(1320)$  ( $\Gamma \sim 107 MeV$ ) and a strange isodoublet  $K_2^*(1430)$  ( $\Gamma \sim 100 MeV$ ). The first isoscalar decays mainly into pions while the second decays mainly into strange mesons. Thus it is natural to infer that the  $f_2(1270)$  is mainly  $u\bar{u} + d\bar{d}$  while the  $f_2'(1525)$  is mainly  $s\bar{s}$ . We have a clear nonet of tensor mesons and we note that the splittings are exactly what one would expect from a mass-difference between strange and non-strange (constituent) quarks of  $\sim 100 MeV$ . Thus the lightest tensors provide a nice illustration of the quark model at its most successful: the mesons fall into  $SU(3)$  multiplets with a modest symmetry breaking driven by the  $m_s - m_n$  mass difference. (For convenience we shall adopt the shorthand notation  $n\bar{n}$  for  $\frac{1}{\sqrt{2}}(u\bar{u} + d\bar{d})$  in the following.)

We now turn to the  $0^{++}$  mesons. The easiest such meson to see experimentally should be the strange isodoublet and the lightest such state turns out to be the  $K_0^*(1430)$  with  $\Gamma \sim 290 MeV$ . Note that this is close in mass to the corresponding tensor although, as expected, its decay width is much larger. (This is what makes the scalars very much harder to identify experimentally.) There is also a candidate isovector  $a_0(1450)$  ( $\Gamma \sim 270 MeV$ ). In addition there are two isoscalars, the  $f_0(1370)$  ( $\Gamma \sim 300 - 500 MeV$ ) and the  $f_0(1500)$  ( $\Gamma \sim 120 MeV$ ). The former decays mainly into pions and so one would suppose it to be composed mainly of non-strange quarks.

So far all this looks much like the tensor nonet. However there is a puzzle. The  $f_0(1500)$  does *not* have the obvious decays for a predominantly  $s\bar{s}$  state. Moreover if we compare its width to the other scalars then we see that it is remarkably narrow - particularly for a state with, apparently, a large non-strange component. This motivates us to look for other nearby scalar states. There is evidence that the  $f_J(1710)$  is, or contains, a  $0^{++}$  state. Moreover the predominant 2-body decays of this state involve strange quarks ( $K\bar{K}$  or  $\eta\eta$ ). The state is relatively narrow  $\Gamma \sim 175 MeV$ . So if we include this state into our discussion, we no longer have an obvious  $s\bar{s}$  problem. However now we have three isoscalar states in the  $1370 - 1710 MeV$  mass region - too many for a quark model nonet! Since, as we have seen, lattice calculations predict a scalar glueball in the  $1600 MeV$  mass region, with a width comparable to that which we observe for the  $f_0(1500)$  and  $f_J(1710)$ , it is natural to conjecture that the three observed isoscalars are in fact the results of mixing between two quarkonium isoscalars and the lightest scalar glueball. This is the scenario explored in [23, 21, 22] with some differing assumptions.

All this might be a convincing picture if it were not for the existence of some lighter scalar states that we have so far failed to mention. These are the isoscalar  $f_0(980)$  and the isovector  $a_0(980)$ . Both are narrow ( $\Gamma \sim 40 - 100 MeV$ ). (There may also be an extremely wide isoscalar in the  $400 - 1200 MeV$  mass range.) Since there is no nearby strange isodoublet, these states certainly do not fit into the usual quark picture where mesons should fall into approximate  $SU(3)$  multiplets with modest symmetry breakings driven by the  $m_s - m_n$  mass difference. In fact these mysterious states were interpreted some time ago [24] as

being loosely-bound  $K\bar{K}$  molecules - recall that they are narrow and occur very close to the  $K\bar{K}$  threshold. If we accept this interpretation - and it has been widely accepted as being plausible - then we can ignore these states for our purposes and the interpretation of the previous paragraph remains. I should stress that alternative interpretations of this spectrum do exist, but I will ignore these here and instead refer you to [4] for a detailed discussion.

The picture we are thus led to is one where the  $f_0(1370)$ , the  $f_0(1500)$  and the  $f_0(1710)$  are the result of mixing between the glueball and the would-be  $s\bar{s}$  and  $n\bar{n}$  scalar quarkonia. We argued above that these quarkonia belong to the same nonet so the  $s\bar{s}$  will be heavier than the  $n\bar{n}$ . Moreover the relative strengths of the glueball mixings will be determined on symmetry grounds.

What are the constraints on the mixing?

First the output masses of the mixing should correspond to the  $f_0(1370)$ ,  $f_0(1500)$  and  $f_0(1710)$ . The first state is very broad and so we shall allow its mass to lie in the region  $M_1 \in [1.31, 1.40]GeV$  with a preference for  $1.37GeV$ . The second state is both quite narrow and well-defined and so we fix its mass to  $M_2 = 1.5GeV$ . The third state appears to be again quite narrow but the precise location of the  $0^{++}$  component is still quite uncertain. We shall consider the range  $M_3 \in [1.64, 1.80]GeV$  with a preference for  $1.71GeV$ .

There are also some constraints on the input parameters. Given the lattice predictions, a generous range for the glueball mass would be  $m_G \in [1.40, 1.80]GeV$ . We also have a qualitative constraint on the glueball-quarkonium matrix element of the Hamiltonian: it should be small,  $\sim O(100)MeV$  or less. Similarly we expect a glueball to be narrow, and so any state with a large glueball component should be narrower than one would otherwise expect. As for the quarkonia, we expect  $m_{s\bar{s}} > m_{n\bar{n}}$ , with a mass difference in the  $\sim 150 - 200MeV$  ballpark. And the mixing matrix elements should be close to their  $SU(3)_{flavour}$  values. There are further, and important, constraints that arise from the observed decays of the three output states and again I refer to [4] for a more detailed discussion.

Here I shall give one example of what appears to be an acceptable mixing scheme. We assume that prior to mixing what we have are the ‘bare’ quarkonia with masses  $m_{s\bar{s}} = 1.61GeV$  and  $m_{n\bar{n}} = 1.36GeV$  and a bare glueball with mass  $m_G = 1.48GeV$ . These are not eigenstates of  $H$  and so the mass matrix will not be diagonal. We can write the latter as

$$\begin{pmatrix} m_G & z & \sqrt{2}z \\ z & m_{s\bar{s}} & 0 \\ \sqrt{2}z & 0 & m_{n\bar{n}} \end{pmatrix}$$

(The factor of  $\sqrt{2}$  follows from the fact that  $\frac{1}{\sqrt{2}}\{\langle u\bar{u}| + \langle d\bar{d}| \}H|G\rangle = \sqrt{2}\langle u\bar{u}|H|G\rangle$ .) The physical masses, after mixing, are the eigenvalues of this mass matrix. With an acceptably weak mixing of  $z = 62MeV$  we obtain as output masses  $1.31, 1.50, 1.64GeV$  for the  $f_0(1370)$ ,  $f_0(1500)$  and  $f_0(1710)$ , which is perfectly acceptable. The overlaps of the output states can be written in terms of the bare input states as follows:

$i$	$f_{in}$	$f_{is}$	$f_{iG}$
$f_0(1370)$	0.87	0.10	-0.49
$f_0(1500)$	0.48	-0.43	0.77
$f_0(1710)$	0.13	0.90	0.42

We see that most of the glueball resides in the  $f_0(1500)$  and the  $f_0(1710)$  is mainly an  $s\bar{s}$  quarkonium. Such a mixing scheme is qualitatively compatible with the observed decays of the output states. This and other possible mixing scenarios are discussed in [4] For some other recent discussions of mixing in this context see [21, 22]

## 2.4 Conclusion

We now know quite accurately the lightest scalar glueball mass in the pure gauge theory in units of the string tension. If we translate this into physical units, as described in this lecture, we find that the glueball should appear around  $\sim 1.60 \pm 0.15 GeV$ . This is just the mass range where one naively expects the two scalar flavour singlet quarkonia to lie. If they do then all these states will inevitably mix to some extent, even though we expect the dynamical mixing parameter to be weak. It is therefore intriguing that experimentally not only are there definitely states in this mass range, the  $f_0(1370)$  and the  $f_0(1500)$ , but there is evidence for a third, the  $f_0(1710)$ . We presented a sample mixing scheme in which the glueball mainly resides in the  $f_0(1500)$ . This is not a new suggestion [21]. While it is still a little too early to come to a convincing conclusion, it certainly seems that it will not be very long before we are able to do so.

I have emphasised the scalar glueball because that is where most of the recent interest has been. What about the tensor and pseudoscalar? In looking for glueball candidates experimentalists naturally look for states that appear in ‘gluon-rich’ processes. For example in  $J/\psi$  decays, or in Pomeron-Pomeron collisions, or states that have large  $\eta\eta$  decays. This picks out the  $f_0(1500)$  and  $f_0(1710)$  amongst the scalars. Amongst the tensors this picks out the  $f_2(1900)$  and the  $G(2150)$ . These are, of course, in the right ball-park for the  $2^{++}$  glueball as predicted by lattice calculations:  $\sim 2.26 \pm 0.22 GeV$ . So here too, things look interesting.

With the pseudoscalar, on the other hand, we have little reason to feel smug. First, the lattice calculations are poor: a mass estimate of  $\sim 2.16 \pm 0.32$  barely qualifies as an estimate at all. Moreover the obvious experimental candidate is the  $\iota(1490)$  seen in  $J/\psi$  decays. We should however remember that this state is special: it has the quantum numbers of the vacuum topological charge. Which brings me smoothly to my next topic.

## 3 Topological fluctuations

As you know,  $SU(N)$  gauge fields in 3+1 dimensions possess a topological charge. [25]. And it is the topological fluctuations of the gauge fields that are the reason why the  $\eta'$  has a mass  $\sim 1 GeV$  rather than being almost a Goldstone boson [26]. Moreover there is good reason to think that these fluctuations lead to the spontaneous breaking of chiral symmetry. The reason is that isolated instantons produce zero modes in the Dirac operator; these mix with each other, and shift away from zero, when the instantons are not isolated (as in the real vacuum). It is not hard to imagine that this might leave a non-zero density of modes

close to zero, and this would suffice to break chiral symmetry (via the Banks-Casher formula [27]). This occurs explicitly in some instanton models (see Shuryak's lectures at this School and [28, 30]) and has been observed in some lattice calculations [29]. It is also possible that instantons may affect the properties of some hadrons, as the near-zero modes may lead to large contributions to the valence-quark propagators. This is more speculative. All this to say that topology is interesting. In addition it is intrinsically non-perturbative. Here I will tell you some things that we have learned by studying topology in lattice gauge theory.

The first thing I need to address is the fact that when we discretise space-time we lose topology in a formal sense, since any field on a discrete set of points can be smoothly deformed to a trivial field. One should not get too excited about this; the same happens with dimensional regularisation. If the space-time dimension is not exactly 4 we have no topological winding. Since the theory is renormalisable we expect that, as the cut-off is removed,  $a \rightarrow 0$ , we recover all the properties of the continuum theory. We shall see how this occurs for topology in the lattice gauge theory.

So in this lecture I will address the following topics. First I discuss the basic ambiguity with defining topology on a lattice; and show why it does not really matter. Then I discuss the practical problem of calculating the topological charge of fields that have fluctuations on all length scales. This is a large subject and I will focus simply on the one technique that goes by the name of 'cooling'. I will then move onto the first bit of physics: the Witten-Veneziano formula that relates the strength of the topological fluctuations in the pure gauge theory to the mass of the  $\eta'$  in QCD. Finally I will attempt to give some insight into the structure of the topological fluctuations in the vacuum.

### 3.1 A basic ambiguity and why it does not matter

Let me start by giving an explicit example. A lattice gauge field is defined by a set of  $SU(2)$  matrices on the links,  $l$ , of the lattice:  $\{U_l\}$ . (I will stick here to  $SU(2)$  for simplicity.) Consider now the following continuum gauge potential for an instanton of size  $\rho$  centered at  $x = 0$ :

$$A_\mu^I(x) = \frac{x^2}{x^2 + \rho^2} g^{-1}(x) \partial_\mu g(x) \quad (12)$$

with

$$g(x) = \frac{x_0 + ix_j \sigma_j}{(x_\mu x_\mu)^{1/2}} \quad (13)$$

Let us now translate this field by  $a/2$  in each direction so that it is centered at  $\bar{x} = (a/2, a/2, a/2, a/2)$ , i.e at the centre of a lattice hypercube. Define a lattice field by:

$$U_\mu^I(x) = \mathcal{P} \exp \int_x^{x+a\hat{\mu}} A_\mu^I(x) dx \quad (14)$$

For  $\rho \gg a$  the lattice discretisation is very fine compared to the instanton core in which the instanton action and topological charge density,  $Q(x) = \frac{1}{32\pi^2} \epsilon_{\mu\nu\rho\sigma} Tr\{F_{\mu\nu}(x)F_{\rho\sigma}(x)\}$ , reside.

In this case any reasonable definition of the topological charge (see below for an example) will assign a topological charge of  $Q = 1$  to this lattice field. Suppose we now continuously reduce  $\rho$ . The lattice field will also vary continuously. Eventually we will have  $\rho \ll a$ . At this stage the instanton core, which is at the centre of a lattice hypercube, will be very far, in units of its size, from any of the lattice links. Thus even the nearest link matrices on the lattice will be arbitrarily close to pure gauge. That is to say, the field configuration will be the same as that due to a gauge singularity located at  $x = \bar{x}$ . In this case any reasonable definition of the topological charge will assign a topological charge of  $Q = 0$  to this lattice field. Thus we have passed continuously from a field with  $Q = 1$  to one with  $Q = 0$ .

Does this raise a fundamental problem with topology on the lattice? The answer is: not really. At least if we are interested, as here, with the limit  $a \rightarrow 0$ . Let me argue why this is so.

Consider the density of topological fluctuations as a function of their size  $\rho$ . This is only an unambiguous notion if  $\rho \ll \xi_d$  where  $\xi_d$  is the typical dynamical length scale of the theory (e.g. 1 fermi in QCD or the inverse mass gap in the pure gauge theory). In that case we know the density of these ‘instantons’:

$$D(\rho)d\rho = \frac{d\rho}{\rho} \frac{1}{\rho^4} e^{-\frac{8\pi^2}{g^2(\rho)}} \dots \quad (15)$$

where the ‘...’ represent factors varying weakly with  $\rho$ . You recognise in this equation the scale-invariant integration measure; also a factor to account for the fact that a ball of volume  $\rho^4$  can be placed in  $1/\rho^4$  different ways in a unit volume; and finally a factor arising from the classical instanton action,  $S_I = 8\pi^2/g^2$ , with perturbative fluctuations promoting the bare  $g^2$  to a running  $g^2(\rho)$  in the usual way. This last sentence is the most important one for us here: if we substitute for  $g^2(\rho)$  in eqn 15 we find that

$$D(\rho)d\rho \propto \rho^6 d\rho \quad : SU(3) \quad (16)$$

with a power  $\rho^{7/3}$  in the case of SU(2). So, because of the scale anomaly, the number of instantons rapidly vanishes as  $\rho \rightarrow 0$  rather than diverging as  $1/\rho^5$ .

On the lattice this density will change as follows if  $a \ll \rho$  and  $a \ll \xi_d$ :

$$D(\rho) \rightarrow D(\rho) \times \left\{ 1 + 0\left(\frac{a^2}{\rho^2}\right) \right\} \quad (17)$$

Now, suppose a lattice field configuration is to be smoothly deformed from  $Q = 1$  to  $Q = 0$ . This requires a topological fluctuation to be squeezed out of the lattice, as described above. While we do not know much about the structure of the original fluctuation (it will typically be on a size scale  $\sim \xi_d$  which is beyond the reach of our analytic techniques) we do know that if the lattice spacing is sufficiently small then to reach  $\rho \sim a$  the ‘instanton’ will have to pass through sizes  $\xi_d \gg \rho \gg a$ . In this region the density is calculable as we saw above, with a probability that is very strongly suppressed; at least as  $\sim (\rho/\xi_d)^6$  for SU(3). So the changing of  $Q$  is conditional upon the involvement of field configurations whose probability  $\rightarrow 0$  as  $a \rightarrow 0$ . Thus, as we approach the continuum limit this lattice ambiguity vanishes very rapidly. We knew that this had to happen because the theory is renormalisable and the lattice is surely a good regulator. It is, however, nice to see it happen explicitly.

## 3.2 Cooling

Having convinced you that it makes sense to discuss topology on the lattice, I now want to discuss how you can calculate it. The obvious ways are three.

- Calculate the zero-modes of the Dirac operator  $\mathcal{D}[A]$ .  $Q$  will equal the difference between the number of left and right handed zero-modes.
- Interpolate a smooth gauge potential. If  $Q \neq 0$  and if space-time is compact (as it is here: a hypertorus) then we will need more than one patch. The net winding of the transition functions between the patches equals  $Q$ .
- We calculate the topological charge density  $Q(x) = \frac{1}{32\pi^2} \epsilon_{\mu\nu\rho\sigma} \text{Tr}\{F_{\mu\nu}(x)F_{\rho\sigma}(x)\}$ . Then  $Q = \int Q(x)d^4x$ .

All these methods have been explored in lattice calculations. I will focus on the last because it is the simplest and because it immediately tells us something about the size and location of the core of the ‘instanton’ (since that is where  $Q(x)$  is localised).

We need a lattice operator that becomes  $Q(x)$  in the continuum limit. This is easy. Recall (see Chris Michael’s lectures) that if we define the plaquette matrix,  $U_{\mu\nu}(x)$ , as the ordered product of link matrices around the corresponding plaquette of the lattice, then it is easy to see that  $U_{\mu\nu}(x) = 1 + a^2 F_{\mu\nu}(x) + \dots$  and hence that [31]

$$Q_L(x) \equiv \frac{1}{32\pi^2} \epsilon_{\mu\nu\rho\sigma} \text{Tr}\{U_{\mu\nu}(x)U_{\rho\sigma}(x)\} = a^4 Q(x) + 0(a^6). \quad (18)$$

If we apply this formula to an instanton of size  $\rho$  (discretised as described above) then we find, as expected, that  $Q_L = \int Q_L(x)dx = 1 + 0(a^2/\rho^2)$ .

Applied to the real vacuum however  $Q_L(x)$  has problems. The operator is dimensionless and so  $0(a^6)$  actually means terms like  $\sim a^6 F^3$ ,  $\sim a^6 F D^2 F$  etc. For smooth fields these are indeed  $0(a^6)$ . However realistic fields (those that contribute to the path integral) have fluctuations all the way up to frequencies of  $0(1/a)$ . So if we take matrix elements of  $Q_L(x)$  in the vacuum the contribution of the high frequency modes to the  $0(a^6)$  terms will be  $\delta Q_L(x) \sim a^6 \times 1/a^6 \sim 0(a^0)$ . In practice this contribution is suppressed by some powers of  $\beta$  that can be calculated in perturbation theory (since these contributions are short-distance). Thus in the real world  $Q_L(x)$  possesses interesting topological contributions that are of order  $a^4 \propto e^{-c\beta}$  (since  $g^2(a) \propto 1/\log(a\Lambda)$ ) and uninteresting ultraviolet contributions that are  $\propto 1/\beta^n$ . So as we approach the continuum limit,  $\beta \rightarrow \infty$ , the latter dominate and we are in trouble.

Actually things are a little worse than this. Like other composite lattice operators,  $Q_L(x)$  possesses a multiplicative lattice renormalisation factor:  $Z_Q \simeq 1 + c'/\beta + \dots$  [32]. This looks innocuous, and indeed in the continuum limit it obviously is. However it turns out that the value of  $c'$  is such that  $Z_Q \ll 1$  precisely in the range of values of  $\beta$  where current lattice calculations are performed.

There are different ways to deal with these problems. I will describe a particularly simple technique [33]. The idea rests on the observation that the problems are all caused by the

ultraviolet fluctuations on wavelengths  $\sim a$ . By contrast, if we are close to the continuum limit, the topology is on wavelengths  $\rho \gg a$ . One can therefore imagine taking the lattice fields and locally smoothing them over distances  $\gg a$  but  $\ll \rho$ . Such a smoothing would erase the unwanted ultraviolet fluctuations while not significantly disturbing the physical topological charge fluctuations. One could then apply the operator  $Q_L(x)$  to these ‘cooled’ fields to reveal the topological charge distribution of the vacuum.

How do we cool a lattice gauge field? The simplest procedure is to take the field and generate from it a new field by the standard Monte Carlo heat bath algorithm subject to one crucial modification: we always choose the new link matrix to locally minimise the plaquette action. Since  $Tr U_{\mu\nu}(x)$  measures the variations of the link matrices over a distance  $a$ , minimising the plaquette action is a very efficient way to erase the ultraviolet fluctuations. (Obviously there are many possible variations on this theme.)

Thus the notion is that we take our ensemble of  $N$  gauge fields,  $\{U^{I=1,\dots,N}\}$ , perform a suitable number of cooling sweeps on each one of these, so obtaining a corresponding ensemble  $\{U_c^{I=1,\dots,N}\}$  of cooled fields, and then extract the desired topological properties from these cooled fields. As one might expect there are ambiguities for realistic values of  $a$ . As we cool, topological charges of opposite sign will gradually annihilate. This changes the topological charge density but not the total value of  $Q$ . Eventually this leads to a very dilute gas of instantons. As we cool even further these isolated instantons will gradually shrink and will eventually shrink within a hypercube and at this point even  $Q$  will change. (This is for a plaquette action on a large enough volume: other actions may have other effects.) Of course when an instanton becomes narrow it has a very peaked charge density and is impossible to miss. So we certainly know when it disappears out of the lattice and can, if we think it appropriate, correct for that. All this to say that cooling is a good way to calculate the total topological charge, but is not necessarily a reliable way to learn about the topological charge density.

Let me give you an example of how it works. I have produced a sequence of 90 Monte Carlo sweeps on a  $12^4$  lattice at  $\beta = 2.5$ . These field configurations are separated by just one heat bath sweep (i.e. each link matrix has been changed only once) so one expects the long distance physics on neighbouring field configurations to be almost identical. That is, the value of  $Q$  should change little. In Fig. 5 I show you the values of  $Q_L$  when calculated on these fields. They jump all over the place and are nowhere near the expected integer values. Now let us cool each of these 90 configurations with 25 cooling sweeps. Calculating  $Q_L$  on these one finds a dramatic difference - as shown in Fig. 5. (The cooled charges differ from integers because there is an  $O(a^2/\rho^2)$  error which is substantial for our not-so-small choice of  $a$ .)

We now have a technique for calculating the topological charge of a lattice field. As we have seen, its application requires some care. Another reason to take care is the following. The probability of instantons with  $\rho \sim a$  depends on the lattice discretisation. If the lattice action is much less than the continuum action then even when  $a \rightarrow 0$  there may be a finite density (per unit physical volume) of these lattice artifacts. They might survive a couple of cooling sweeps. For realistic values of  $a$  the gap in scales between  $a$  and  $\xi_d$  is not very large and so such a narrow instanton, if sitting on a background field due to a physical but

moderately narrow anti-instanton, might expand under cooling rather than shrinking. So it might occasionally survive our 20, or whatever, cooling sweeps and bias our calculations. Obviously this latter effect disappears as  $a \rightarrow 0$ . Another correction is due to the fact that with finite  $a$  one loses the tail of the continuum density that extends to  $\rho \leq a$ . This correction also disappears as  $a \rightarrow 0$ . To deal with these problems one needs to perform a suitable scaling analysis. For example suppose we define a topological charge  $Q_L(\rho_c)$  which only includes topological charges for which  $\rho \geq \rho_c = an_c$ . As  $a \rightarrow 0$   $Q_L(\rho_c)$  should become independent of  $\rho_c$  for a growing range  $n_c^{min} \leq n_c \leq n_c^{max}$ : with  $an_c^{min}$  large enough to exclude any  $\rho \sim a$  artifacts and  $n_c^{max}$  growing exponentially with  $\beta$ . We shall demonstrate a simple calculation of this kind next.

### 3.3 The topological susceptibility

Since  $\langle Q \rangle = 0$  (we have no  $\theta$ -term) the simplest quantity we can calculate is  $\langle Q^2 \rangle$ . However there is a much better reason for calculating it: it is directly related [34, 35] to the  $\eta'$  mass:

$$\chi_t \equiv \frac{\langle Q^2 \rangle}{volume} \simeq \frac{f_\pi^2}{2N_f} (m_{\eta'}^2 + m_\eta^2 - 2m_K^2) \quad (19)$$

If we put in the experimental numbers into the above formula, then we get

$$\chi_t \sim (180 \text{ MeV})^4 \quad (20)$$

In this relation the susceptibility,  $\chi_t$ , is that of the pure gauge theory - which is something that we can calculate. We now describe such a calculation and see what happens.

The values of  $\langle Q^2 \rangle$  that I am going to use come from calculations that I have done in the past; for SU(3) they come from [36, 37] while for SU(2) they come from [38, 39, 40]. All these calculations have been performed using 20 to 25 cooling sweeps. The charge  $Q_L$  is then calculated on these cooled lattice fields. This charge is non-integer because the smallest instanton charges suffer significant  $O(a^2/\rho^2)$  corrections. However such small instantons have very peaked densities and are easy to identify. One can then estimate the corrections due to these small instantons, and shift  $Q_L$  to the appropriate integer topological charge  $Q$ . This has been done in all these calculations.

In Fig. 6 I plot  $\chi_t/\sqrt{\sigma}$  against the string tension,  $a^2\sigma$  in lattice units. We expect the leading lattice corrections to this dimensionless mass ratio to be  $O(a^2/\rho^2)$ , as in eqn 1. So we would attempt a continuum extrapolation of the form

$$\frac{\chi_t(a)}{\sqrt{\sigma(a)}} = \frac{\chi_t(0)}{\sqrt{\sigma(0)}} + ca^2\sigma \quad (21)$$

which is a simple straight line on the plot. As we see the calculated values are consistent with this functional form. In addition to the susceptibility calculated from the total charge we also calculate  $Q$  with narrow instantons removed. The particular cut we have used is to remove all charges whose peak density is greater than  $1/16\pi^2$ . This corresponds to removing instantons with  $\rho \leq 3a$ . In doing this we are largely removing lattice artifacts with  $\rho \sim a$



which, because of their environment, survive the cooling. Of course we are also removing a part of the small- $\rho$  tail of the continuum density,  $D(\rho)$ . So we are not saying that this is necessarily a better measure of the continuum susceptibility. What we do wish to check is that both these susceptibilities are consistent when extrapolated to the continuum limit. And as we see in Fig. 6 this is indeed so. We extract:

$$\lim_{a \rightarrow 0} \frac{\chi_t}{\sqrt{\sigma}} = 0.437 \pm 0.020 \pm 0.015 \quad (22)$$

Here the first error is statistical and the second is a systematic error estimated using the two different extrapolations. If we now plug in our favourite value for the string tension,  $\sqrt{\sigma} = 440 \text{ MeV}$ , we obtain

$$\chi_t = (192 \pm 12 \text{ MeV})^4 \quad (23)$$

Of course we should really incorporate the uncertainty in the value of  $\sqrt{\sigma}$ , most of that coming from setting MeV units, and this would increase the error to  $\pm 20 \text{ MeV}$ . Irrespective of such details it is clear that the pure gauge theory susceptibility is indeed consistent with being large enough to drive the large  $\eta'$  mass.

In Fig. 7 I show the corresponding plot for the  $SU(2)$  susceptibility. Again we see that the two susceptibilities we calculate are consistent when extrapolated to the continuum limit. Note that the difference between the two at corresponding values of  $a$  is much greater for  $SU(2)$  than for  $SU(3)$ . This is because the  $SU(N)$  running coupling,  $g^2(\rho)$ , runs much faster to zero as  $N \uparrow$  and so any finite- $a$  ambiguities between physical and ultraviolet topological charges rapidly decrease. We extract:

$$\lim_{a \rightarrow 0} \frac{\chi_t}{\sqrt{\sigma}} = 0.470 \pm 0.011 \pm 0.015 \quad : \quad SU(2) \quad (24)$$

which translates to

$$\chi_t = (207 \pm 9 \text{ MeV})^4 \quad : \quad SU(2) \quad (25)$$

if we use  $\sqrt{\sigma} = 440 \text{ MeV}$ . Unfortunately we do not know the  $\eta'$  etc. masses for the  $SU(2)$  theory so we cannot say if this is what is expected. And neither does it make much sense to introduce MeV units by using the  $SU(3)$  value of  $\sqrt{\sigma}$  in this way. It does however allow me to compare to two recent estimates of  $200 \pm 15 \text{ MeV}$  [41] and of  $230 \pm 30 \text{ MeV}$  [42] which have been obtained using quite different methods, but a similar  $\text{MeV}$  scale. As we see, the values are all consistent - which is reassuring.

### 3.4 Vacuum topological structure

The calculation of  $Q$  on the lattice is relatively straightforward. If we continuously deform a continuum gauge field so as to minimise the action then we necessarily get driven to the semiclassical multi-instanton minimum. We do not change topological charge sectors since these are separated by infinite action barriers. Cooling is just a naive lattice version of this procedure and so it should work in this way for  $a \rightarrow 0$ . As we have seen, it does indeed seem to work well.

However there are other things we would like to know about the instanton density if we are interested in gauging the possible influence of instantons on chiral symmetry breaking, the quarkonium spectrum and related physics. For example a picture in which instantons have a mean size of  $\sim 1/3fm$  and are relatively dilute produces a plethora of interesting physics [28]. Can we say something about such more detailed features of the vacuum topological structure?

This question involves both technical and conceptual ambiguities. There are two main technical problems. The first is that as we cool a gauge field its topological structure changes: instantons will change their sizes and nearby instantons and anti-instantons will annihilate. These quantities are not invariant under minimising the action; they are not even quasi-stable. So we must do as little cooling as possible and trust only those features that we find to be relatively insensitive to cooling. If the vacuum that one obtains is a dilute gas of instantons then there is no further difficulty. However what one might expect, and indeed finds, is a relatively dense gas of overlapping charges. This raises a difficult problem of pattern recognition, particularly for the larger instantons whose density,  $Q_L(x)$  will be very small (it obviously varies as  $1/\rho^4$ ) and which are most likely to overlap with several other large instantons. Such large instantons will, in any case, not be completely smooth, and may possess multiple peaks ('ripples') since we are trying to minimise the number of cooling sweeps used. These problems have been addressed in different ways by several recent calculations of this kind [43, 41, 42, 44, 45]. I think it is fair to say that all these should be regarded as exploratory. However, to whet your appetite I am going to show you some results from an analysis that I have been involved in [45]. What I am not going to do here is to tell you anything at all about the pattern recognition algorithms etc.

I mentioned a conceptual difficulty. Instantons are semiclassical objects. The real vacuum has fluctuations on all scales and there is no reason to think that the topological charge resides in instanton-like objects. Does it even make sense to talk of a distribution in  $\rho$ ? This raises all kinds of interesting questions, including: do we care? After all, models such as that in [28] would not claim to be more than simplifications that are appropriate to the physics being considered. Perhaps we should regard a minimal amount of smoothening as performing such a simplification upon the fluctuating gauge fields? I am not going to address these questions any further here, but you should be aware of their existence.

Let me now move to some results of this kind of calculation [45]. The calculations are in the pure SU(3) gauge theory. We have used lattice fields that have been generated and stored (for other purposes) by the UKQCD Collaboration. We are performing calculations on  $16^3 48$  and  $32^3 64$  lattices at  $\beta = 6.0$ ,  $24^3 48$  lattices at  $\beta = 6.2$ , and  $32^3 64$  lattices at  $\beta = 6.4$ . The point of the 2 lattice sizes at  $\beta = 6.0$  is to check for finite volume effects - especially for the very large instantons. The various lattice spacings enable us to check whether the features we identify have the right scaling properties to survive into the continuum limit. In addition we do the calculations for various different numbers of cooling sweeps so that we can check whether these features are insensitive to cooling or not.

In Fig. 8 I show the size distribution,  $D(\rho)$ , with the size  $\rho$  expressed in units of  $1/\sqrt{\sigma} \equiv 1/\sqrt{K}$ . The peak is around  $\rho \sim 0.5fm$ . This is not very sensitive to  $\beta$  or to the lattice size or to the number of cooling sweeps. The total number of charges is of course sensitive to the

amount of cooling. We do, however, note that unless we go to a very large number of cools, the vacuum is dense with a great deal of overlap between the charges.

It is not straightforward to test for scaling, since a cooling sweep is intrinsically non-scaling. What we do find is that if we tune the number of cooling sweeps so that the total number of charges is independent of  $\beta$ , then the detailed densities,  $D(\rho)$ , seem to scale as well.

Two other aspects of  $D(\rho)$  are of particular interest: the fall-offs at small and large  $\rho$ . The former is interesting because it provides a check on our calculations: we know that  $D(\rho) \propto \rho^6$  for  $a \ll \rho \ll 1/\sqrt{\sigma}$ . Of course we can only approach these severe inequalities by looking for the trend as we increase  $\beta$ . We do indeed find a tendency to approach something close to this functional behaviour. (Which, in any case, is modified by powers of  $\log \rho$ .) By contrast large  $\rho$  is interesting because we do not know what happens to large instantons in a confining vacuum. If we used the semiclassical formula with a coupling that froze at large  $\rho$  then we would get  $D(\rho) \propto 1/\rho^5$  as  $a \rightarrow \infty$ . What we find is a much stronger suppression:

$$D(\rho) \propto \frac{1}{\rho^{\sim 11}} \quad : \quad \rho \gg \frac{1}{\sqrt{\sigma}} \quad (26)$$

Before closing this subject let me move to a quite different and more subtle aspect of the vacuum structure. In a dilute gas the correlation between the sign of a charge and the sign of the total charge will be independent of size  $\rho$ . In Fig. 9 I show the correlation we actually find. There is a striking size-dependence. Charges smaller than average tend to have the same sign as  $Q$ , larger charges tend to have the opposite charge. Since the sign of  $Q$  simply tells you which sign wins out on that configuration, this tells us that net charge of the small instantons wins out over the net charge of the larger instantons. This suggests a picture where the very large instantons are polarised, so that the small instantons sitting on this background tend to have the opposite charge throughout the volume. Since the charge of the small instantons wins out, this means that the large instantons are actually overscreened. Of course this would be a lot to glean from the one plot; however this intriguing picture is in fact supported by more detailed calculations. It leads to quite striking effects. Suppose for example we decide to calculate the total charge that includes instantons smaller than some value  $\rho_c$ :  $Q_{\rho \leq \rho_c}$ . The fluctuations are shown in Fig. 10. We note that if we were to limit ourselves to instantons with  $\rho \leq 1/\sqrt{\sigma}$  then we would obtain a topological susceptibility that is  $\sim 10$  times greater than the total susceptibility! It is clearly important to investigate the effect of these structures on quark propagators and hence on the observable physics.

### 3.5 Conclusions

In this lecture I hope that I have convinced you that simulations of lattice gauge theories can be both useful and interesting in telling us something about the topological fluctuations of the vacuum. Some of what I have shown you, particularly concerning the long distance polarisation of the vacuum, must be regarded as preliminary - to a potentially embarrassing degree. The calculations of the topological susceptibility, on the other hand, are now quite reliable. They show us that the topological vacuum fluctuations are indeed large enough to

drive the large  $\eta'$  mass. The theoretical expectations with which we compared our result arise, most straightforwardly, from arguments about what happens in  $SU(N)$  QCD at large  $N$ . This takes me smoothly to the final of my three topics in these lectures.

## 4 $SU(N_c)$ gauge theories for all $N_c$

Quantum Chromodynamics is an  $SU(3)$  gauge theory coupled to 3 lightish quark colour triplets. If we change the gauge group to  $SU(2), SU(4), SU(5), \dots$  then we obtain an infinite set of, a priori, quite different theories. However from an analysis of Feynman diagrams to all orders [46] one finds that the  $N_c \rightarrow \infty$  limit of such  $SU(N_c)$  theories is smooth if we vary the coupling as  $g^2 \propto 1/N_c$ . This suggests that it should be possible to describe  $SU(N_c)$  gauge theories as perturbations in powers of  $1/N_c$  around  $SU(\infty)$  [46], at least for large enough  $N_c$ . Moreover if one assumes confinement for all  $N_c$ , then one can easily show [46, 47] that the phenomenology of the  $SU(\infty)$  quark-gluon theory is strikingly similar to that of (the non-baryonic sector of) QCD. This makes it conceivable that the physically interesting  $SU(3)$  theory could be largely understood by solving the much simpler  $SU(\infty)$  theory. If all the  $SU(N_c)$  theories down to  $SU(3)$  can be treated in this way, then this represents an elegant and enormous theoretical simplification.

I do not have the time to review [48] this subject here, but let me at least indicate something of what is involved, albeit using arguments that lack any rigour. The constraint that  $g^2 \propto 1/N_c$  is easy to motivate. Consider inserting a gluon loop into a gluon propagator. We have added two triple-gluon vertices and this gives a factor  $g^2$ . At the same time the sum over colour in the loop gives a factor of  $N_c$ . (Not  $N_c^2$  because the colour of the incoming/outgoing gluon is fixed.) So we have a total factor  $\sim g^2 N_c$ . Now such loops can be inserted any number of times, so if we want a smooth large- $N_c$  limit (at least in all-order perturbation theory) then we clearly need to impose  $g^2 \propto 1/N_c$ . Assume therefore that we have done so. Consider a typical meson decay, e.g.  $\rho \rightarrow \pi\pi$ . This requires the production of a  $q\bar{q}$  pair. So the decay width contains a factor of  $g^2 \propto 1/N_c$ . But if we have confinement all the hadrons are colour singlets and so we do not acquire any compensating factors from summing over the colours of the decay products. Thus the decay width is suppressed by a factor  $1/N_c$ . That is, at large  $N_c$  hadrons do not decay. This is like a ‘narrow-width’ caricature of the real world. In fact this is a reasonable first approximation to the hadrons we know; mostly their widths are very much smaller than their masses. A similar argument tells us that mixings, e.g. between mesons and glueballs, are suppressed. This is reminiscent of the OZI rule discussed in my first lecture. This (and much more) suggests that the  $SU(\infty)$  theory is indeed a first approximation to  $SU(3)$ .

All this motivates us to try and answer by explicit calculation some basic questions:

- does a non-perturbative calculation support the (all-orders) perturbative argument for a smooth  $N_c \rightarrow \infty$  limit?
- is  $N_c \rightarrow \infty$  confining?

- does such a limit really require  $g^2 \propto 1/N_c$ ; and if so what does this mean when we have a running coupling?
- is  $SU(N_c) \simeq SU(\infty)$  only for  $N_c \gg 1$  or is it the case down to  $N_c = 3$ , or even  $N_c = 2$ ?
- what is the  $SU(\infty)$  mass spectrum?

There have been a number of interesting computational explorations of the lattice  $SU(\infty)$  theory (for a review see [49]) based on the fact that it can be re-expressed as a single plaquette theory [50]. Unfortunately this scheme makes no statement about the size of the leading corrections to the  $N_c = \infty$  limit, and so gives us no clue as to how close  $N_c = 3$  is to  $N_c = \infty$ .

In this lecture I will describe an extremely straightforward approach to this problem. I will simply calculate the properties of  $SU(N_c)$  gauge theories for several values of  $N_c$  and so determine explicitly how the physics varies as  $N_c$  increases. I will only look at the pure gauge theory, but there are good reasons for believing that the inclusion of quarks will not alter any of our conclusions (except in some obvious ways). Ideally I would like to present you with accurate calculations in 4 dimensions. Unfortunately, at present what I can provide you there is very rough and tentative. But I will make up for that by describing the results of the corresponding, but much more precise, calculation in 3 dimensions. Of course you will want to know what is the relevance of such a ‘substitution’. I will come to that shortly.

My study was originally motivated by the observation that the  $C = +$  sector of the light mass spectrum turned out to be quite similar in the  $D = 2 + 1$   $SU(2)$  [51, 52] and  $SU(3)$  [53] theories. (This also appears to be the case in  $D = 3 + 1$ , although there the comparison is weakened by the much larger errors.) One reason for this might be that both are close to the  $N_c = \infty$  limit. In that case we would have an economical understanding of the spectra of  $SU(N_c)$  gauge theories for all  $N_c$ : there is a common spectrum with small corrections.

A second, more practical reason for studying  $N_c \rightarrow \infty$  was my interest in obtaining some model understanding of the structure of glueballs. Models are of interest even if they are very approximate in comparison with the results of simulations. A good model will embody the essential degrees of freedom in a problem and show how this leads to the main features of the physics, within some transparent and plausible approximation scheme. A model could provide the intuition necessary for an economical understanding of the role of glueballs in a wide range of contexts. For example, if one understands the structure of glueballs, one can make crude but reliable estimates of glueball-quarkonium mixing, of glueball decay, of the effects of dynamical quarks etc. In many cases the approximations made in the model include the neglect of decays and mixing. These are features of the  $SU(\infty)$  rather than of the  $SU(3)$  theory, and so it would be better to test the model against the spectrum of the former theory. One example that has been of particular interest to me is the flux tube model of glueballs [54, 55, 56]. The formulation of this model is identical for all  $N_c > 2$ . However, because the model does not incorporate the effects of glueball decay, it should presumably be tested against the  $N_c \rightarrow \infty$  spectrum since it is only in that limit that there are no decays. It is also the case that many theoretical approaches are simpler in that limit. An example is provided by the recent progress in calculating the large  $N_c$  mass spectrum using light-front quantisation techniques [57].

The  $D = 2 + 1$  analysis that I shall present here is based on my calculations over the last few years of the properties of  $SU(N_c)$  gauge theories with  $N_c = 2, 3, 4$  and  $5$ . In  $D = 3 + 1$  what I have done is to perform some  $SU(4)$  calculations to supplement what is known about  $SU(2)$  and  $SU(3)$ . My strategy is the very simple one of directly calculating the mass spectra of these theories and seeing whether they are approximately independent of  $N_c$ . The calculations are performed through the Monte Carlo simulation of the corresponding lattice theories, using the standard plaquette action. In the  $D = 2 + 1$  case the calculations are very accurate and we are able to extrapolate our mass ratios to the continuum limit prior to the comparison. In the  $3+1$  dimensional case our  $SU(4)$  calculations are not good enough for that, and our comparisons with  $SU(2)$  and  $SU(3)$  are correspondingly less precise. Some of the  $SU(2)$  results have been published [51, 52] as have brief summaries of the results discussed here [58, 59]. A long paper is in preparation.

#### 4.1 $D=2+1 \sim D=3+1$ ?

While one might naively expect that the  $D = 2 + 1$  and  $D = 3 + 1$  gauge theories would be so different as to make a unified treatment misleading, this is not in fact so. Theoretically the  $D = 2 + 1$  theory shares with its  $D = 3 + 1$  homologue four important properties.

- Both theories become free at short distances. In 3 dimensions the coupling,  $g^2$ , has dimensions of mass so that the effective dimensionless expansion parameter on a scale  $l$  will be

$$g_3^2(l) \equiv l g^2 \xrightarrow{l \rightarrow 0} 0 \quad (27)$$

In 4 dimensions the coupling is dimensionless and runs in a way we are all familiar with:

$$g_4^2(l) \simeq \frac{c}{\ln(l\Lambda)} \xrightarrow{l \rightarrow 0} 0 \quad (28)$$

In both cases the interactions vanish as  $l \rightarrow 0$ , although they do so much faster in the super-renormalisable  $D = 2 + 1$  case than in the merely asymptotically free  $D = 3 + 1$  case.

- Both theories become strongly coupled at large distances. This we see immediately by letting  $l \uparrow$  in the above formulae. Thus in both cases the interesting physics is nonperturbative.
- In both theories the coupling sets the mass scale. In 3 dimensions it does so explicitly:

$$m_i = c_i g^2 \quad (29)$$

In 4 dimensions it does so through the phenomenon of dimensional transmutation: the classical scale invariance is anomalous, the coupling runs and this introduces a mass scale through the rate at which it runs:

$$m_i = c_i \Lambda \quad (30)$$

- Both theories confine with a linear potential. This is not something that we can prove by a simple argument. However lattice simulations provide convincing evidence that this is indeed the case. Note that although the  $D = 2 + 1$  Coulomb potential is already confining,

this is a weak logarithmic confinement,  $V_C(r) \sim g^2 \ln(r)$ , which has nothing to do with the nonperturbative linear potential,  $V(r) \simeq \sigma r$ , that one finds at large  $r$ .

In addition to these theoretical similarities, the calculated spectra also show some striking similarities.

- In both theories the lightest glueball is the scalar  $0^{++}$  with a similar mass  $m_{0^{++}} \sim 4\sqrt{\sigma}$ . In the  $C = +$  sector, the  $2^{++}$  is the next lightest glueball (ignoring any excited scalars) with  $m_{2^{++}}/m_{0^{++}} \sim 3/2$  in both cases.

All this motivates us to believe that a unified treatment makes sense.

Of course there are significant differences as well. For example:

- There are no instantons in  $D = 2 + 1$  non-Abelian gauge theories. This probably implies quite different quark physics.
- The rotation group is Abelian.
- The details of the mass spectrum are very different in 3 and 4 dimensions. A particularly striking difference is that in 3 dimensions the spectrum exhibits parity doubling for states with non-zero angular momentum:

$$m_{J^+} = m_{J^-} \quad \text{if } J \neq 0 \tag{31}$$

This follows from the fact that angular momentum flips sign under parity - which can be defined in  $D = 3$  as  $(x, y) \rightarrow (-x, y)$ . The proof is elementary and I leave it as an exercise. Actually to show this you need the continuum rotation group. If you only have  $\pi/2$  rotations then you find that you lose parity doubling for the  $J = 2$  state. This can happen either because you are too close to the strong coupling limit or because the volume is too small and the rotation symmetry is broken by the boundary conditions. In either case this is a useful check: that we are effectively in the continuum limit and in an effectively infinite volume.

## 4.2 2+1 dimensions.

The calculations in 3 dimensions are performed in the same way as in 4 dimensions except that the computational problem is much more manageable. (Lattices grow as  $L^3$  rather than as  $L^4$ .) The basic steps are just as outlined in my first lecture, and you will have to trust me that all the checks have been performed sufficiently carefully! After extrapolating to the continuum limit I obtain the string tension and a mass spectrum in units of  $g^2$ . Only the lightest portion of the mass spectrum is calculated, but that includes  $J^{PC}$  states for  $J = 0, 1, 2$  and  $P = \pm$  and  $C = \pm$  as well as one or two further excited states in many cases. I do this for  $SU(2)$ ,  $SU(3)$ ,  $SU(4)$  and  $SU(5)$ . In the case of  $SU(2)$  there is no  $C = -$  sector. In fact the main point of the  $SU(5)$  calculation was to have 3 values of  $N_c$  for the  $C = -$  states, so as to provide some control over their  $N_c$  dependence. The  $SU(5)$  calculation is recent and has not been incorporated into the analysis that follows.

I begin with the string tension,  $\sigma$ , since it turns out to be our most accurately calculated physical quantity. We use smeared Polyakov loops [38], to obtain  $a^2\sigma$  for several values of

the lattice spacing  $a$ . We then extrapolate the lattice results, using the asymptotic relation  $\beta = 4/ag^2$ , to obtain the continuum string tension in units of  $g^2$ :

$$\frac{\sqrt{\sigma}}{g^2} = \lim_{\beta \rightarrow \infty} \frac{\beta}{2N_c} a \sqrt{\sigma} \quad (32)$$

The results for  $SU(2), SU(3)$  and  $SU(4)$  in  $D = 2 + 1$  [58] are shown in Table 1 and are plotted in Fig. 11. We immediately see that there is an approximate linear rise with  $N_c$  and we find that we can obtain a good fit with

$$\frac{\sqrt{\sigma}}{g^2} = 0.1974(12)N_c - \frac{0.120(8)}{N_c}. \quad (33)$$

We obtain a similar behaviour with the light glueball masses (see below).

Some observations.

- For large  $N_c$ , eqn 33 tells us that  $\sqrt{\sigma} \propto g^2 N_c$ . That is to say, the overall mass scale of the theory, call it  $\mu$ , is proportional to  $g^2 N_c$ . In other words, in units of the mass scale of the theory

$$g^2 \propto \frac{\mu}{N_c}. \quad (34)$$

While this coincides with the usual expectation based on an analysis of Feynman diagrams, we note that here the argument is fully non-perturbative.

- The string tension is non-zero for all  $N_c$  and, in particular, for  $N_c \rightarrow \infty$  (when expressed in units of  $g^2 N_c$  or the lightest glueball masses - see below). This confirms the basic assumption that needs to be made in 4 dimensions in order to extract the usual phenomenology of the large- $N_c$  theory.

- In the pure gauge sector one expects (again from an analysis of Feynman diagrams) [48] that the first correction to the large- $N_c$  limit will be  $O(1/N_c^2)$  relative to the leading term. The fit in eqn 33 is indeed of this form. We note that if we try a fit with a  $O(1/N_c)$  correction instead (which would be appropriate if we had quarks) then we obtain an unacceptably poor  $\chi^2$  (corresponding to a confidence level of only  $\sim 2\%$  in contrast to the  $\sim 45\%$  we obtain for the quadratic correction). We may regard this as providing some non-perturbative support for this diagram-based expectation.

- The coefficient of the correction term in eqn 33 is comparable to that of the leading term, suggesting an expansion in powers of  $1/N_c$  that is rapidly convergent. Indeed one has to go to  $N_c = 1$  before the correction term becomes comparable to the leading term. While the  $SU(1)$  theory is completely trivial, we note that the  $U(1)$  theory has a zero string tension (in the sense that  $\sqrt{\sigma}/g^2 = 0$  in the continuum limit).

Let me now turn from the string tension to the mass spectrum. Recall that since we are in  $D = 2 + 1$ , states of opposite parity are degenerate as long as  $J \neq 0$ . This degeneracy is broken by lattice spacing and finite volume corrections. I will present the results separately for the  $P = +$  and  $P = -$  states so as to provide an explicit check on the presence of any such unwanted corrections.



I begin with the  $C = +$  spectrum since the  $SU(2)$  spectrum does not contain  $C = -$  states. In this case we have masses for three values of  $N_c$ , and so can check how good is a fit of the kind in eqn 33. In Fig. 12. I plot the ratio  $m_G/g^2N_c$  against  $1/N_c^2$  for a selection of the lightest states,  $G$ . On this plot a fit of the form in eqn 33. will be a straight line and I show the best such fits. As we can see, the data is consistent with such a  $1/N_c^2$  correction being dominant for  $N_c \geq 2$ . However what is really striking is the lack of *any* apparent  $N_c$  dependence for the lightest  $0^{++}$  and  $2^{++}$  states.

In Table 2 I present the results of fitting the  $C = +$  states to the form

$$\frac{m_G}{g^2N_c} = R_\infty + \frac{R_{slope}}{N_c^2}. \quad (35)$$

where  $R_\infty = \frac{m_G}{g^2N_c} \Big|_{N_c=\infty}$ . (Note that the errors on the slope and intercept are highly correlated.) The confidence levels of the fits are quite acceptable suggesting once again that for  $N_c \geq 2$  a moderately sized correction of the form  $\sim 1/N_c^2$  is all that is needed. Note that since the variation with  $N_c$  is small, the exact form of the correction used will not have a large impact on the extrapolation to  $N_c = \infty$  (except in estimating the errors).

These calculations confirm my earlier claim that the physical mass scale at large  $N_c$  is  $g^2N_c$ . So if we consider ratios of  $m_G$  to  $\sqrt{\sigma}$  (as was explicitly done in [59]) we will find that they have finite non-zero limits as  $N_c \rightarrow \infty$ : that is to say, the large- $N_c$  theory possesses linear confinement.

For the  $C = -$  states we only have masses for 2 values of  $N_c$  and we cannot therefore check whether a fit of the form in eqn 35 is statistically favoured or not. However given that such a fit has proved accurate for the  $C = +$  masses and for the string tension down to  $N_c = 2$  it seems entirely reasonable to assume that it will be appropriate for  $N_c \geq 3$  for the  $C = -$  masses. Assuming this we obtain the results shown in Table 3 for the  $N_c = \infty$  limit and for the coefficient of the first correction. The ‘lever arm’ on this extrapolation is, of course, shorter than for the  $C = +$  states and that leads to correspondingly larger errors. This will be dramatically improved once I incorporate the  $SU(5)$  spectrum into the analysis.

The results in the Tables provide us not only with values for the various mass ratios in the limit  $N_c \rightarrow \infty$  but also, when inserted into eqn 33, predictions for *all* values of  $N_c$ .

Finally, I should remark that I have also calculated the deconfining temperature,  $T_c$ , for  $SU(2)$  [60] and for  $SU(3)$  [53]. Extrapolating as in eqn 33, we find

$$\frac{T_c}{g^2N_c} = 0.1745(52) + \frac{0.079(23)}{N_c^2}. \quad (36)$$

Of course, extrapolating from  $N_c = 2, 3$  is much less reliable than extrapolating from  $N_c = 3, 4$ , and so this relation should be treated with some caution.

### 4.3 3+1 dimensions.

Our knowledge of 4 dimensional gauge theories is much less precise. As far as continuum properties are concerned, quantities that are known with reasonable accuracy include the

string tension, the lightest scalar and tensor glueballs, the deconfining temperature and the topological susceptibility. As in 3 dimensions, the  $SU(2)$  and  $SU(3)$  values are within  $\sim 20\%$  of each other, which encourages us to investigate the  $SU(4)$  theory so as to see whether we are indeed ‘close’ to  $N_c = \infty$ . Of course these  $SU(4)$  calculations are much slower than in  $D = 2 + 1$  and the results I will present here are of a very preliminary nature [58].

I use the standard plaquette action, and so the first potential hurdle is the presence of the well-known bulk transition that occurs as we increase  $\beta$  from strong towards weak coupling. To locate this transition I have performed a scan on a  $10^4$  lattice and found that it occurred at  $\beta = 10.4 \pm 0.1$ . This corresponds to a rather large value of the lattice spacing,  $a$ , and so does not lie in the range of couplings within which we shall be working, i.e.  $\beta = 10.7, 10.9$  and  $11.1$ .

Our calculation consists of 4000, 6000 and 3000 sweeps on  $10^4, 12^4$  and  $16^4$  lattices at  $\beta = 10.7, 10.9$  and  $11.1$  respectively. Every fifth sweep we calculated correlations of (smeared) gluonic loops and from these we extracted the string tension and the masses of the lightest  $0^{++}$  and  $2^{++}$  particles, using standard techniques [38, 10]. These are presented in Table 4. We also calculated the topological susceptibility,  $a^4 \chi_t$ . The charge  $Q$  was obtained using the cooling method discussed in the previous lecture. These calculations were performed every 50 sweeps. Overall this corresponds to rather small statistics and the errors are therefore unlikely to be very reliable.

We see from Table 4 that the most accurate physical quantity in our calculations is the string tension,  $\sigma$ . Can we learn from it how  $g^2$  varies with  $N_c$ , just as we did in  $D = 2 + 1$ ? We focus on a particular embodiment of this question: if we compare different  $SU(N_c)$  theories at a value of  $a$  which is the same in physical units, i.e. for which  $a\sqrt{\sigma}$  is the same, does the bare coupling vary as  $1/N_c$ , i.e. does  $\beta \equiv 2N_c/g^2 \propto N_c^2$ ? We perform this comparison for  $\beta_4 = 10.9, 11.1$ . (For convenience we shall label  $\beta$  by the value of  $N_c$ , i.e. we write it as  $\beta_{N_c}$ .) To find the corresponding values of  $\beta$  in  $SU(2)$  and  $SU(3)$  we simply interpolate between the values provided in (for example) [38, 10]. Doing so we find that the values of  $\beta$  corresponding to  $\beta_4 = 10.9, 11.1$  are  $\beta_3 \simeq 5.972(18), 6.071(24)$  and  $\beta_2 \simeq 2.442(9), 2.485(11)$  respectively. If we simply scale  $\beta_4$  by  $N_c^2$  then what we would expect to obtain is  $\beta_3 \simeq 6.131, 6.244$  and  $\beta_2 \simeq 2.725, 2.775$  respectively. Superficially the numbers look to be in the right ballpark, but in fact the agreement is poor. For example  $\beta_2 = 2.725$  and  $\beta_2 = 2.442$  correspond to values of  $a\sqrt{\sigma}$  that differ by about a factor of 3.

This disagreement should not, however, be taken too seriously, since it is well-known that the lattice bare coupling is a very poor perturbative expansion parameter. It is known that one can get a much better expansion parameter if one uses instead the mean-field improved coupling,  $g_I^2$ , obtained from  $g^2$  by dividing it by the average plaquette,  $\langle \frac{1}{N_c} \text{Tr} U_p \rangle$  [61]. Defining  $\beta_{N_c}^I \equiv 2N_c/g_I^2(a)$  we find that  $\beta_4 = 10.9, 11.1$  correspond to  $\beta_4^I = 6.215, 6.474$  respectively. Scaling  $\beta_4^I$  by  $N_c^2$  we would expect the equivalent  $SU(3)$  and  $SU(2)$  couplings to be given by  $\beta_3^I = 3.496, 3.642$  and  $\beta_2^I = 1.554, 1.619$ . What we actually find is that the equivalent couplings are  $\beta_3^I \simeq 3.527(22), 3.649(28)$  and  $\beta_2^I = 1.561(10), 1.613(12)$ . The agreement is now excellent. That is to say, if the  $SU(N_c)$  mean-field improved bare-coupling is defined on a length scale that is related to the physical length scale ( $\sqrt{\sigma}$ ) by some constant factor, then it varies as  $g^2 \propto 1/N_c$ . This is, of course, the usual diagram-based expectation.

In Fig. 13 I plot the scalar and tensor glueball masses, in units of  $\sqrt{\sigma}$ , as a function of  $N_c$ . For  $N_c = 2, 3$  we have used the continuum values. For  $N_c = 4$  the calculations are not precise enough to permit an extrapolation to the continuum limit and so we simply present the values that we obtained at  $\beta = 10.9$  and  $11.1$ . (We do not use the  $\beta = 10.7$  values since they have large errors and there is the danger that the scalar mass may be reduced by its proximity to the critical point at the end of the bulk transition line.) Although the  $N_c = 4$  errors are quite large, it certainly seems that there is little variation with  $N_c$  for  $N_c \geq 2$  and any dependence appears to be consistent with being given by a simple  $1/N_c^2$  correction. The fact that these mass ratios appear to have finite non-zero limits, implies that the large- $N_c$  theory is confining.

As mentioned earlier we have also calculated the topological susceptibility. In Fig. 14 we plot the dimensionless ratio  $\chi_t^{1/4}/\sqrt{\sigma}$  as a function of  $N_c$ . Once again the  $N_c=2$  and  $3$  values are continuum extrapolations of lattice values, while in the case of  $SU(4)$  we simply display the lattice values obtained at  $\beta=10.9$  and  $11.1$ . As we remarked earlier one expects, semiclassically, very few small instantons for  $SU(4)$  and this is confirmed in our cooling calculations. This has the advantage that the lattice ambiguities that arise when instantons are not much larger than  $a$  are reduced as compared to  $SU(3)$ , and dramatically reduced as compared to  $SU(2)$ . This implies that the interesting large- $N_c$  physics of topology (and the related meson physics) should be straightforward to study.

#### 4.4 Conclusions.

I have shown you the mass spectra and string tensions of gauge theories with  $N_c = 2, 3, 4$  in 3 dimensions. We saw that there is only a small variation with  $N_c$  and that this can be accurately described by a modest  $O(1/N_c^2)$  correction. That is to say, such theories are close to their  $N_c = \infty$  limit for all values of  $N_c \geq 2$ . We also saw that the large- $N_c$  theory is confining and that  $g^2 \propto 1/N_c$  when expressed in physical units. This confirms, in a fully non-perturbative way, expectations arrived at from analyses of Feynman diagrams. It simultaneously provides a unified understanding of all our  $SU(N_c)$  theories in terms of just the one theory,  $SU(\infty)$ , with modest corrections to it. In practical terms this means that, from the parameters in our Tables, we know the corresponding masses for *all* values of  $N_c$ .

Our calculation in 4 dimensions, while quite preliminary, does suggest that the situation may be much the same there. This is obviously something that needs to be done much better. Of particular interest are topological fluctuations at large  $N_c$ : the instanton size density,  $D(\rho)$ , loses its small  $\rho$  tail and lattice topology should become unambiguous. At the same time it would be interesting to investigate the behaviour of hadrons composed of quarks: for example the  $\eta'$  mass should vanish as  $N_c \rightarrow \infty$ . There are many problems of real theoretical interest here. I hope some of you will choose to get involved.

## Acknowledgements

My thanks to Pierre van Baal for inviting me to lecture at this School and for his efforts in making it such a success. I would also like to thank him, David Olive and Peter West for inviting me to the very stimulating Workshop at the Isaac Newton Institute that preceded the School and, finally, the Institute itself for providing such a splendid research environment.

## References

- [1] J.Sexton et al., Phys Rev. Letters, 75 (1995) 4563.
- [2] G.Bali et al, Phys. Lett. B309 (1993) 378.
- [3] H. Chen et al, Nucl. Phys. Proc. Suppl. B34 (1994) 357.
- [4] F. E. Close and M. Teper, inpreparation.
- [5] M. Creutz, Quarks, Gluons and Lattices (CUP 1983).
- [6] I. Montvay and G. Munster, Quantum Fields on a Lattice (CUP 1994).
- [7] M. Luscher, Comm. Math. Phys. 104 (1986) 177; 1983 Cargese Lectures.
- [8] K. Symanzik, Nucl. Phys. B226 (1983) 187.
- [9] D. Perkins, Introduction to High Energy Physics (Addison-Wesley 1987).
- [10] C. Michael and M. Teper, Nucl. Phys. B314 (1989) 347.
- [11] Ph.de Forcrand et al, Phys. Lett. B152 (1985) 107.
- [12] Ph.de Forcrand et al, Phys. Lett. B160 (1985) 137; P. Bacilieri et al, Phys. Lett. B205 (1988) 535; S. Perantonis and C. Michael, Nucl. Phys. B347 (1990) 854; G. Bali and K. Schilling, Phys. Rev. D46 (1992) 2636; Phys. Rev. D47 (1993) 661; S. Booth et al, Nucl. Phys. B294 (1992) 385; C. Allton et al, Nucl. Phys. B407 (1993) 331; H. Wittig, Nucl. Phys. Proc. Suppl. B42 (1995) 288.
- [13] C. Morningstar and M. Peardon, Phys. Rev. D56 (1997) 4043.
- [14] F.Butler et al, Nucl. Phys. B430 (1994) 179.
- [15] R. Kenway et al, Nucl. Phys. Proc. Suppl. B53 (1997) 206; H. Shanahan et al, Phys. Rev. D55 (1997) 1548; S. Ryan, Ph.D. Thesis, Edinburgh 1996.

- [16] W. Lee and D. Weingarten, Nucl. Phys. Proc. Suppl. B53 (1997) 236.
- [17] P. Lacock et al, Phys. Rev. D54 (1996) 6997.
- [18] F. E. Close, Introduction to Quarks and Partons (Academic Press 1979).
- [19] S. Godfrey and N. Isgur, Phys. Rev. D32 (1985) 189.
- [20] Particle Data Group, Phys. Rev. D54 (1996) 1.
- [21] C. Amsler and F. Close, Phys. Rev. D53 (1996) 295.
- [22] D. Weingarten, Nucl. Phys. Proc. Suppl. B53 (1997) 232.
- [23] M. Genovese, Phys. Rev. D46 (1992) 5204.
- [24] R. Jaffe, Phys. Rev. D15 (1977) 267.
- [25] S. Coleman, Aspects of Symmetry, Ch.7 (CUP 1985).
- [26] G. 't Hooft, Physics Reports 142 (1986) 357.
- [27] T. Banks and A. Casher, Nucl. Phys. B169 (1980) 103.
- [28] T. Schaefer and E. Shuryak, hep-ph/9610451.
- [29] S. Hands and M. Teper, Nucl. Phys. B347 (1990) 819.
- [30] N. Dowrick and M. Teper, Nucl. Phys. Proc. Suppl. B42 (1995) 237.
- [31] P. di Vecchia et al, Nucl. Phys. B192 (1981) 392.
- [32] M. Campositrini et al, Phys. Lett. B212 (1988) 206.
- [33] M. Teper, Phys. Lett. B162 (1985) 357.
- [34] E. Witten, Nucl. Phys. B156 (1979) 269.
- [35] G. Veneziano, Nucl. Phys. B159 (1979) 213.
- [36] J. Hoek et al, Nucl. Phys. B288 (1987) 589.
- [37] M. Teper, Phys. Lett. B202 (1988) 553.
- [38] C. Michael and M. Teper, Nucl. Phys. B305 (1988) 453.
- [39] D. Pugh and M. Teper, Phys. Lett. B218 (1989) 326; B224 (1989) 159.
- [40] M. Teper, unpublished.
- [41] P. de Forcrand et al, Nucl. Phys. B499 (1997) 409.
- [42] T. DeGrand, A. Hasenfratz and T. Kovacs, hep-lat/9705009

- [43] C. Michael and P. Spencer, Phys. Rev. D52 (1995) 4691.
- [44] R. Brower et al, Nucl. Phys. Proc. Suppl. 53 (1997) 547.
- [45] D. Smith et al, hep-lat/9709128; in preparation.
- [46] G. 't Hooft, Nucl. Phys. B72 (1974) 461.
- [47] E. Witten, Nucl. Phys. B160 (1979) 57.
- [48] S. Coleman, 1979 Erice Lectures.
- [49] S.R. Das, Rev. Mod. Phys. 59 (1987) 235.
- [50] T. Eguchi and H. Kawai, Phys. Rev. Lett. 48 (1982) 1063.
- [51] M. Teper, Phys. Lett. B289 (1992) 115.
- [52] M. Teper, Phys. Lett. B311 (1993) 223.
- [53] M. Teper, in preparation.
- [54] N. Isgur and J. Paton, Phys. Rev. D31 (1985) 2910.
- [55] T. Moretto and M. Teper, hep-lat/9312035.
- [56] R. Johnson and M. Teper, hep-lat/9709083
- [57] F. Antonuccio and S. Dalley, Nucl. Phys. B461 (1996) 275.
- [58] M. Teper, Phys. Lett. B397 (1997) 223.
- [59] M. Teper, Nucl. Phys. (Proc. Suppl.) 53 (1997) 715.
- [60] M. Teper, Phys. Lett. B313 (1993) 417.
- [61] G. Parisi, in *High Energy Physics - 1980*(AIP 1981); G. Lepage and P. Mackenzie, Phys. Rev. D48 (1993) 2250.

$N_c$	$\sqrt{\sigma}/g^2$
2	0.3350 (15)
3	0.5530 (20)
4	0.7564 (45)

Table 1: The  $D = 2 + 1$   $SU(N_c)$  confining string tension.

$\beta$	$R_\infty$	$R_{slope}$
$\sqrt{\sigma}$	0.1974 ( 12)	-0.12 ( 1)
$0^{++}$	0.805 ( 13)	-0.06 ( 8)
$0^{++*}$	1.245 ( 27)	-0.41 (14)
$0^{-+}$	1.788 ( 88)	-0.48 (56)
$2^{++}$	1.333 ( 29)	-0.08 (18)
$2^{-+}$	1.340 ( 40)	-0.01 (24)
$1^{++}$	1.946 ( 75)	-0.59 (47)
$1^{-+}$	1.919 (115)	-0.18 (75)

Table 2: States with  $C = +$  in  $D = 2 + 1$  :  $R_\infty \equiv \lim_{N_c \rightarrow \infty} \frac{m_G}{g^2 N_c}$  and  $R_{slope}$  is the coefficient of the  $1/N_c^2$  correction in eqn 35.

$G$	$R_\infty$	$R_{slope}$
$0^{--}$	1.18 ( 6)	0.1 (0.6)
$0^{--*}$	1.47 (10)	0.3 (1.1)
$0^{+-}$	1.98 (28)	-0.4 (2.7)
$2^{--}$	1.52 (14)	0.9 (1.4)
$2^{+-}$	1.58 (13)	-0.4 (1.3)
$1^{--}$	1.85 (15)	-0.3 (1.5)
$1^{+-}$	1.78 (23)	1.3 (2.3)

Table 3: As in Table 2 but for states with  $C = -$ .

$\beta$	$a\sqrt{\sigma}$	$am_{0^{++}}$	$am_{2^{++}}$
10.7	0.296 (14)	0.98 (17)	1.78 (34)
10.9	0.229 ( 7)	0.77 ( 8)	1.20 (10)
11.1	0.196 ( 7)	0.78 ( 6)	1.08 (10)

Table 4:  $SU(4)$  in 4 dimensions; masses calculated at the values of  $\beta$  shown.

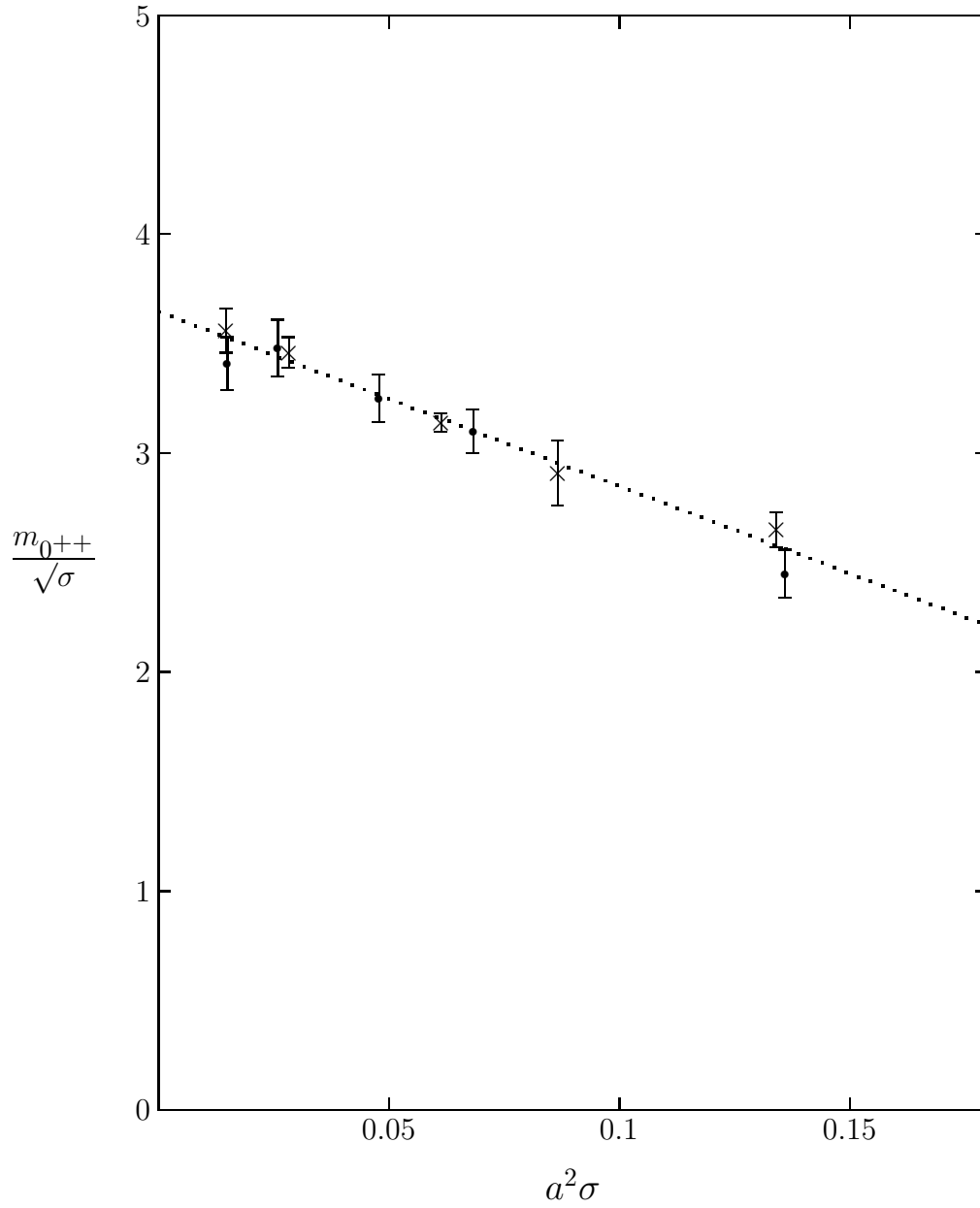


Figure 1: The scalar glueball mass: the GF11 values ( $\times$ ) and the rest ( $\bullet$ ). The best linear extrapolation to the continuum limit is shown.



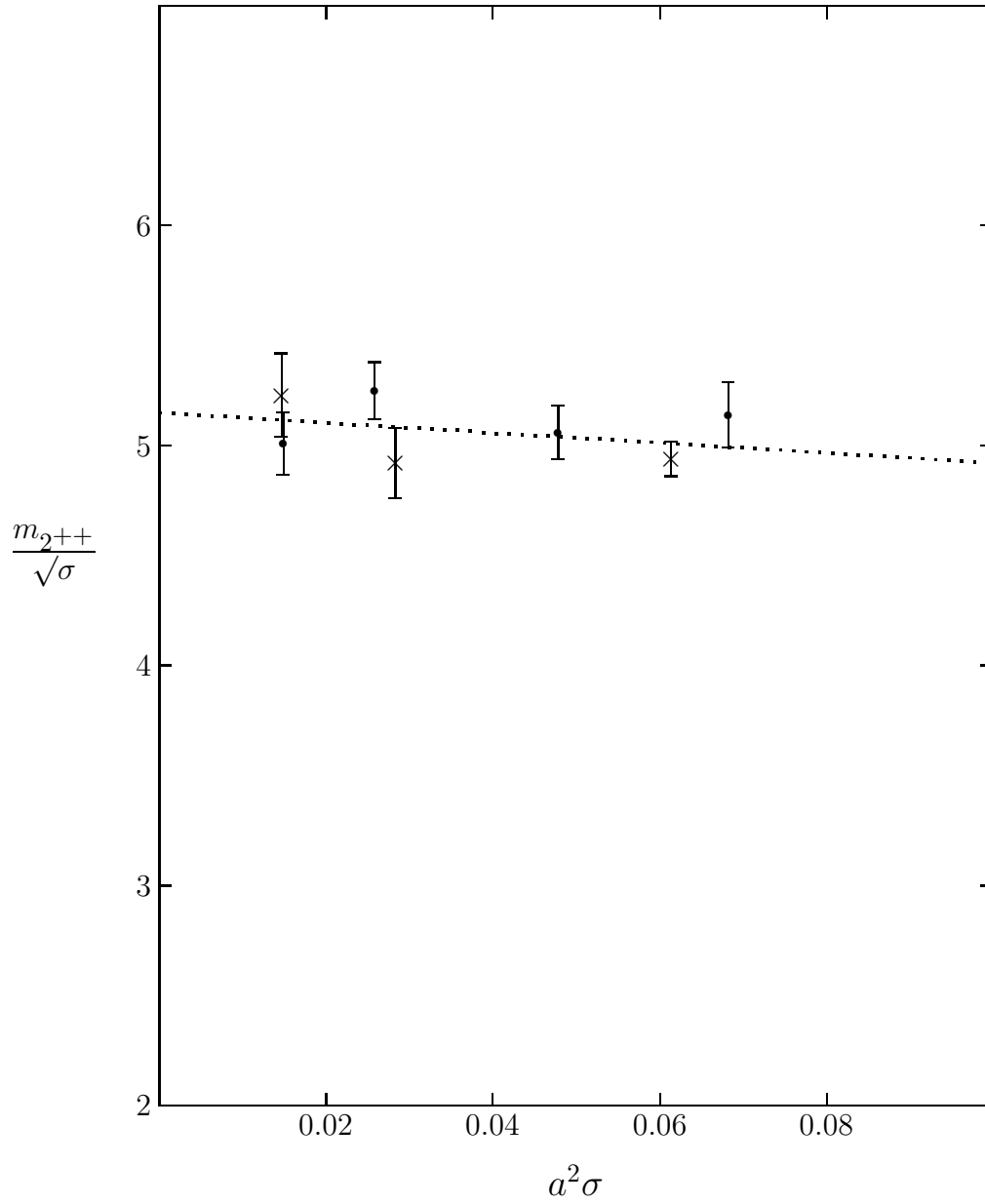


Figure 2: The tensor glueball mass: the GF11 values (×) and the rest (•). The best linear extrapolation to the continuum limit is shown.

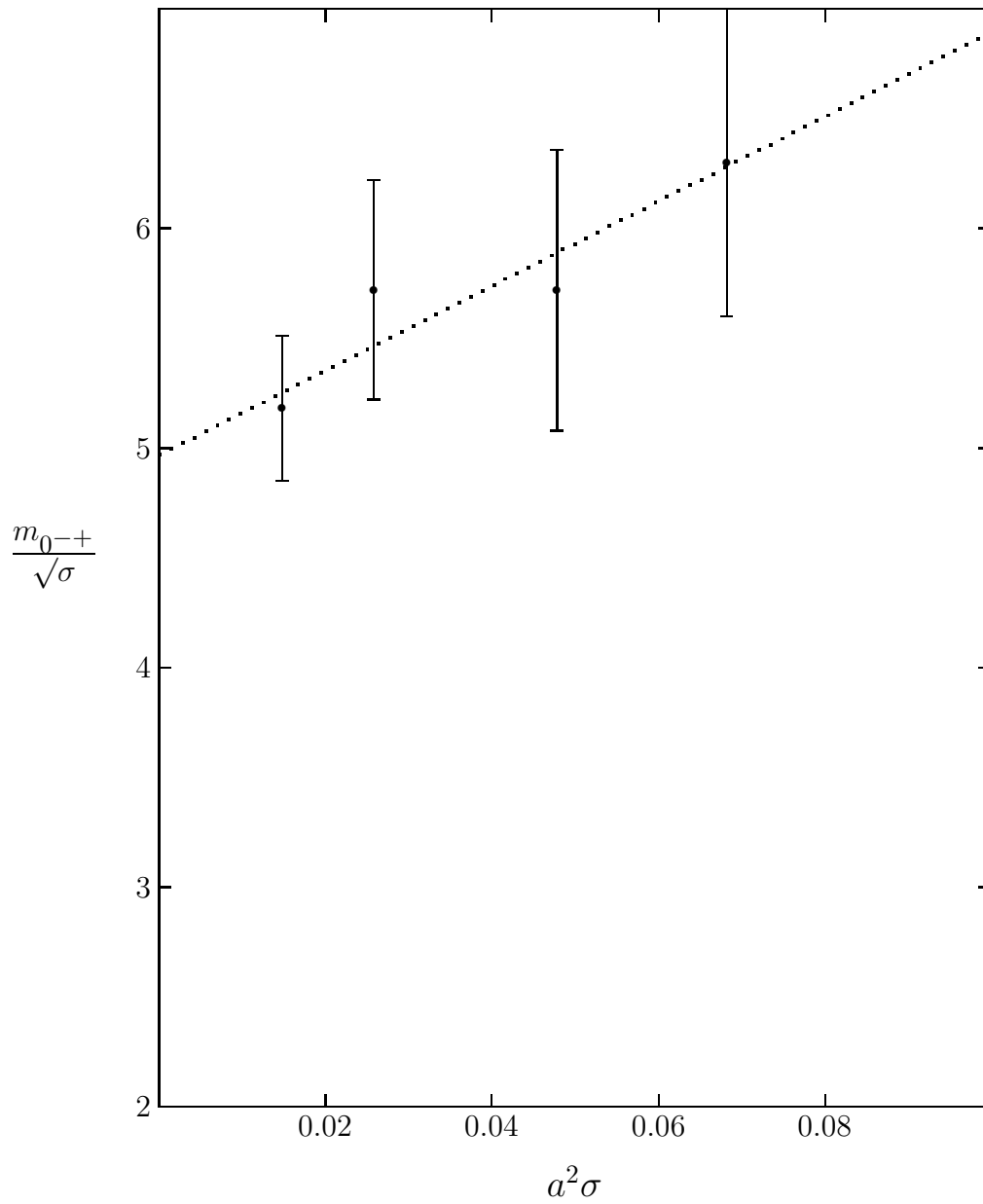


Figure 3: The pseudoscalar glueball mass. The best linear extrapolation to the continuum limit is shown.

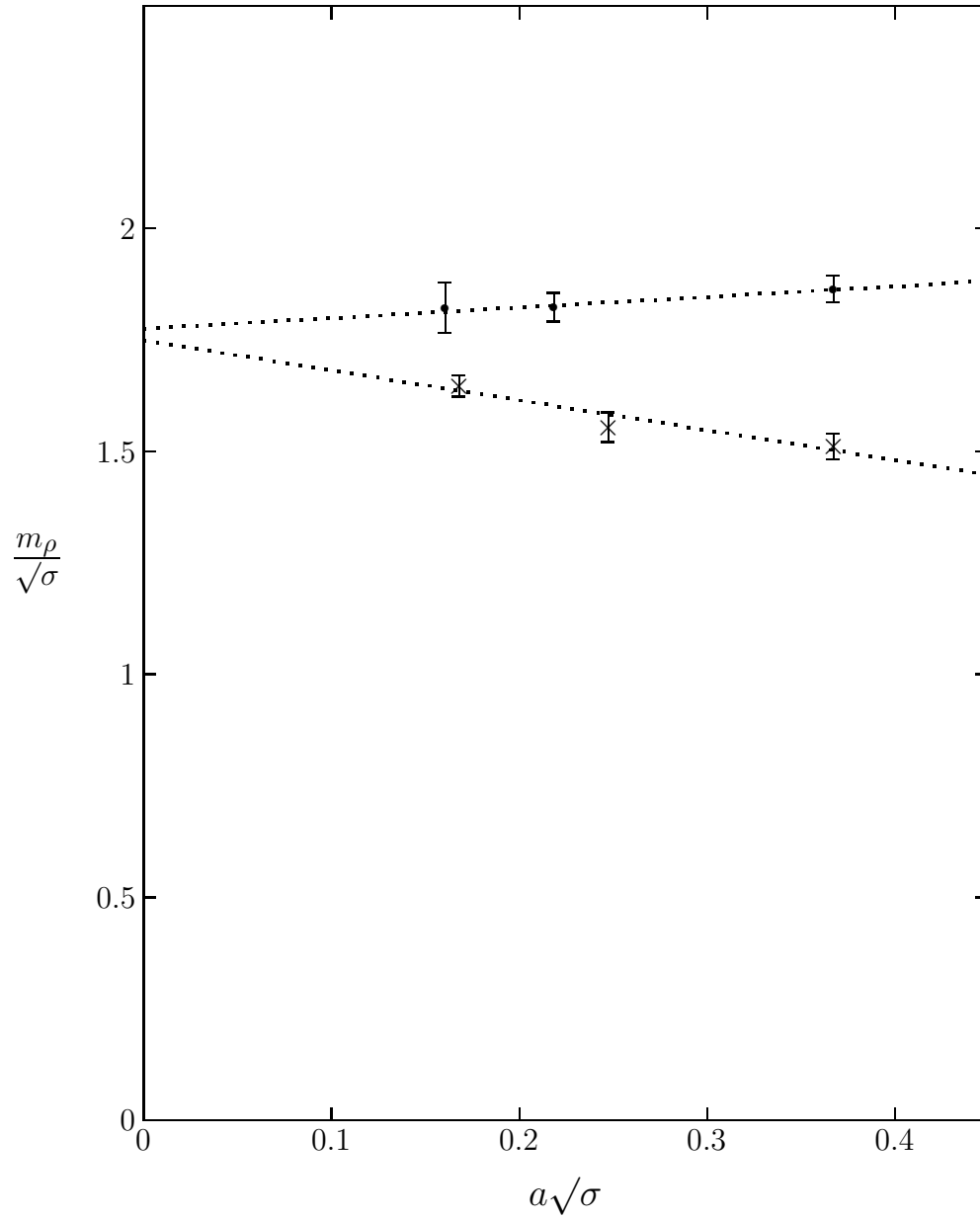


Figure 4: The  $\rho$  mass: GF11 ( $\times$ ) and UKQCD ( $\bullet$ ) values. The best linear extrapolations to the respective continuum limits are shown.

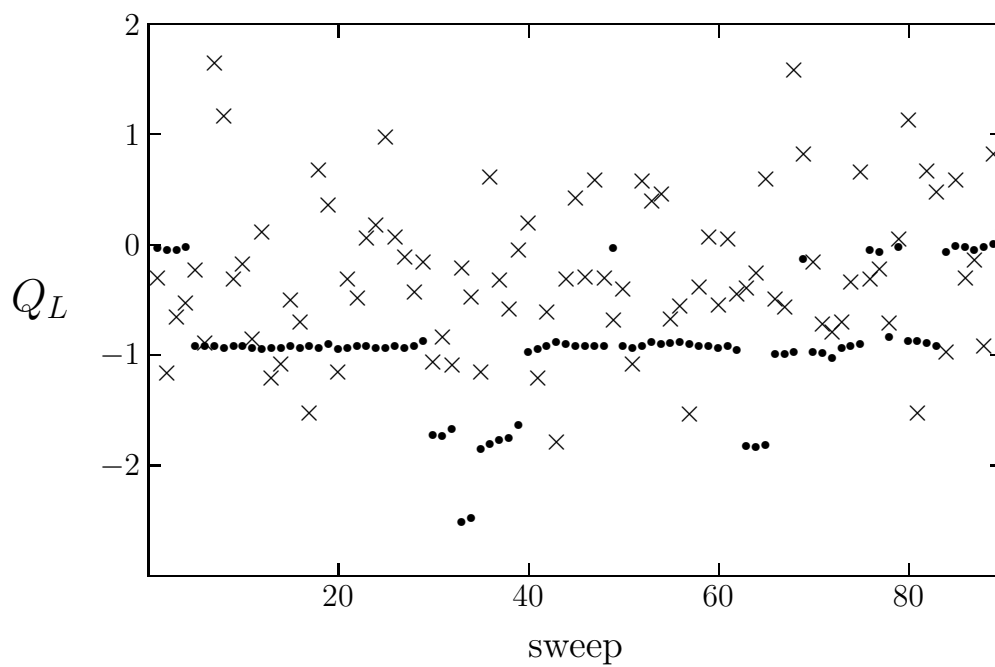


Figure 5: The lattice topological charge: before cooling ( $\times$ ) and after cooling ( $\bullet$ ) the fields. Calculated on a sequence of fields separated by one Monte Carlo sweep.

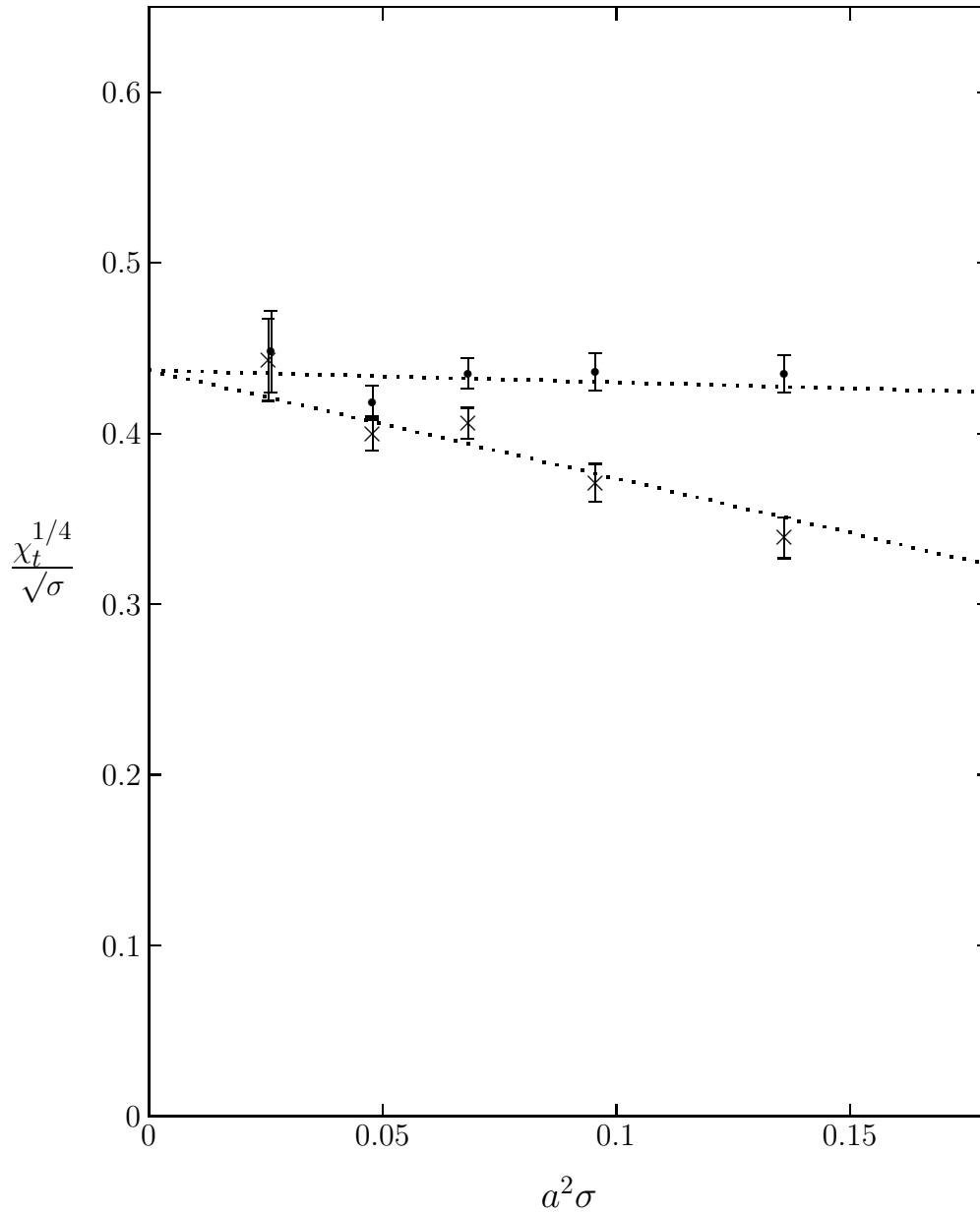


Figure 6: The SU(3) topological susceptibility: from all peaks (●) and from peaks with  $Q(x_{peak}) \leq 1/16\pi^2$  (×). Sample extrapolations to a common continuum limit are shown.

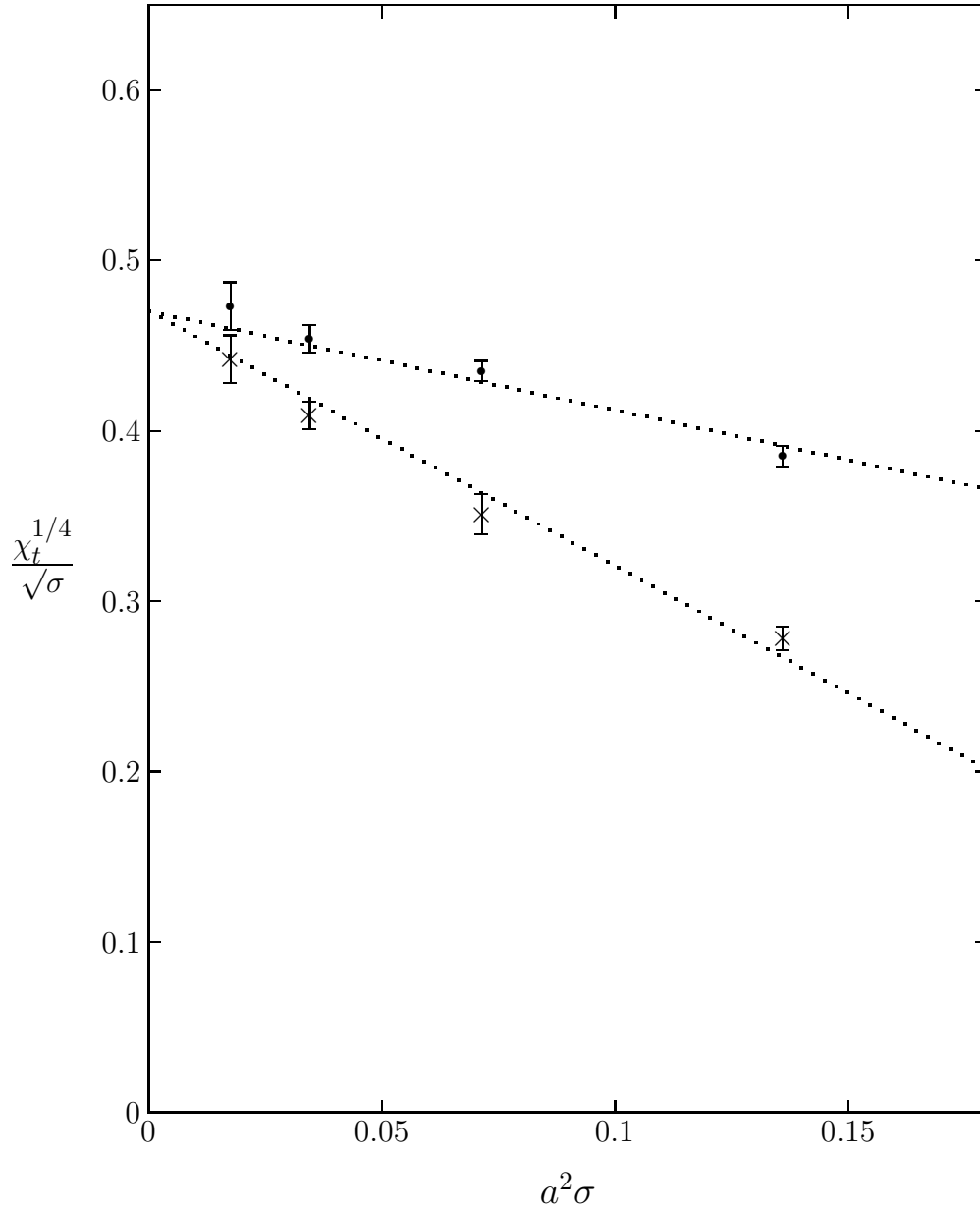


Figure 7: The SU(2) topological susceptibility: from all peaks (●) and from peaks with  $Q(x_{peak}) \leq 1/16\pi^2$  (×). Sample extrapolations to a common continuum limit are shown.

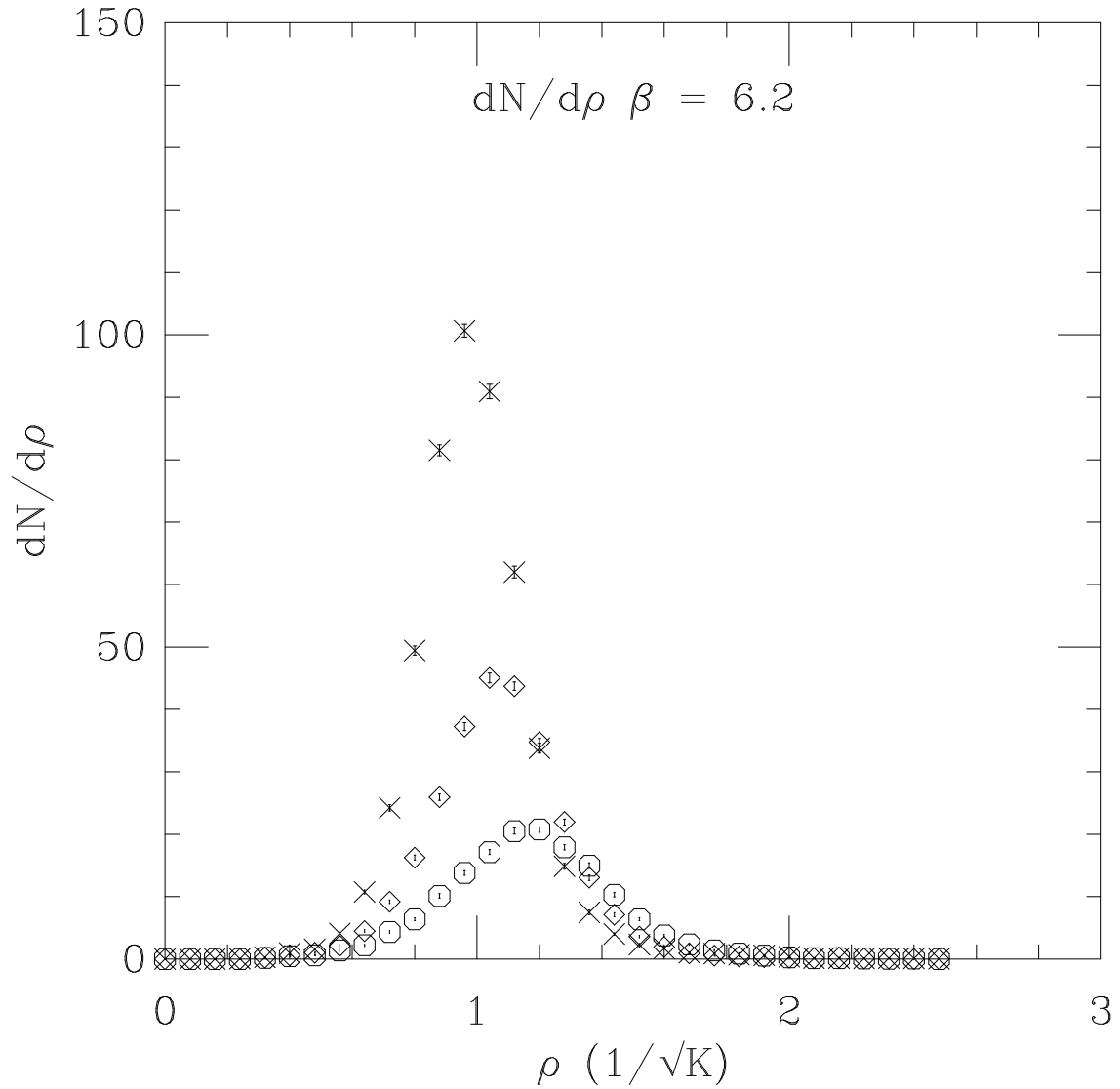


Figure 8: The number of topological charges versus size at  $\beta = 6.2$ : after 23 ( $\times$ ), 32 ( $\diamond$ ) and 46 ( $\circ$ ) (under-relaxed) cooling sweeps. The size is in units of  $1/\sqrt{K}$  where  $K$  is the string tension.

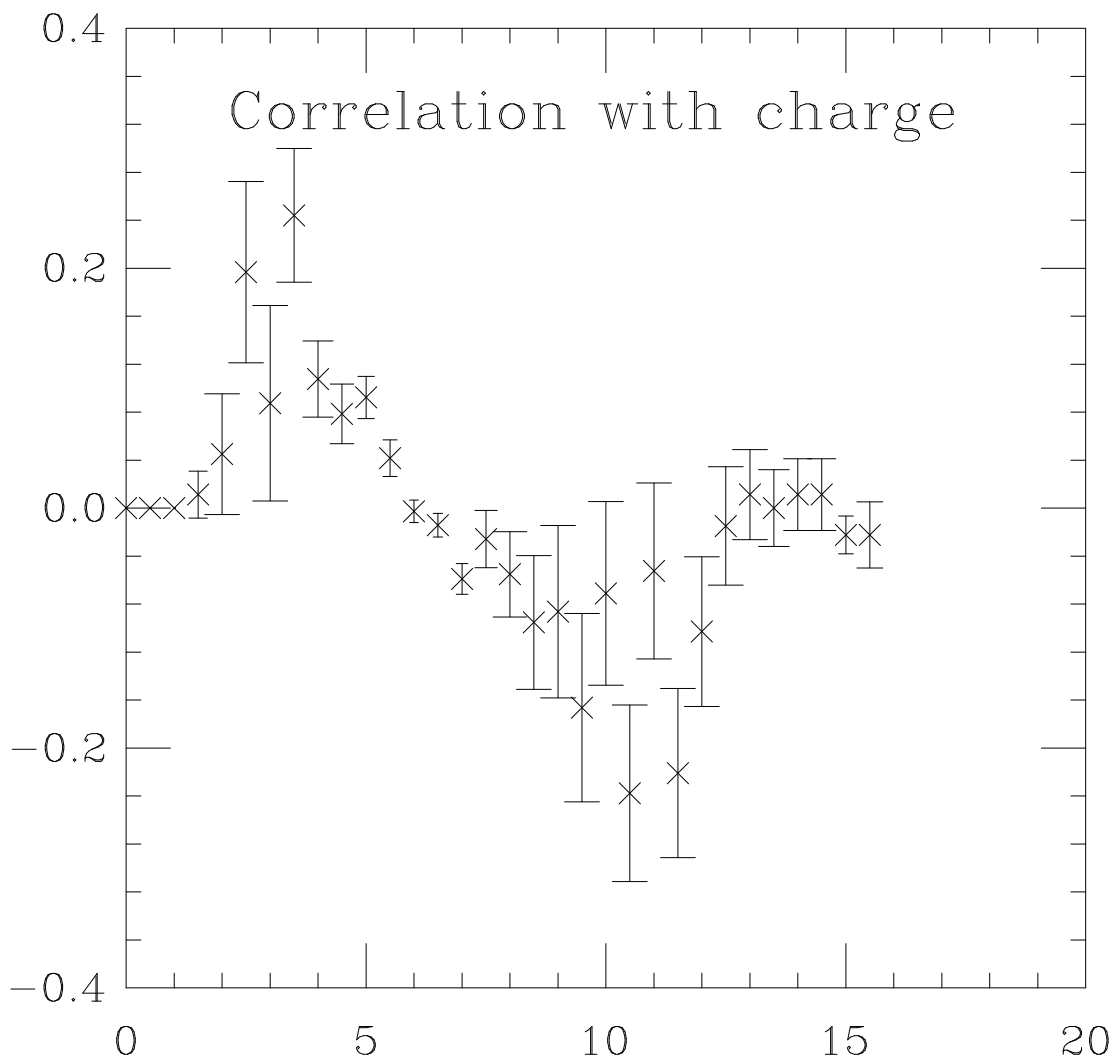


Figure 9: The average correlation between the sign of a charge of size  $\rho$  and the sign of the total charge of the gauge field; at  $\beta = 6.2$  after 23 cooling sweeps



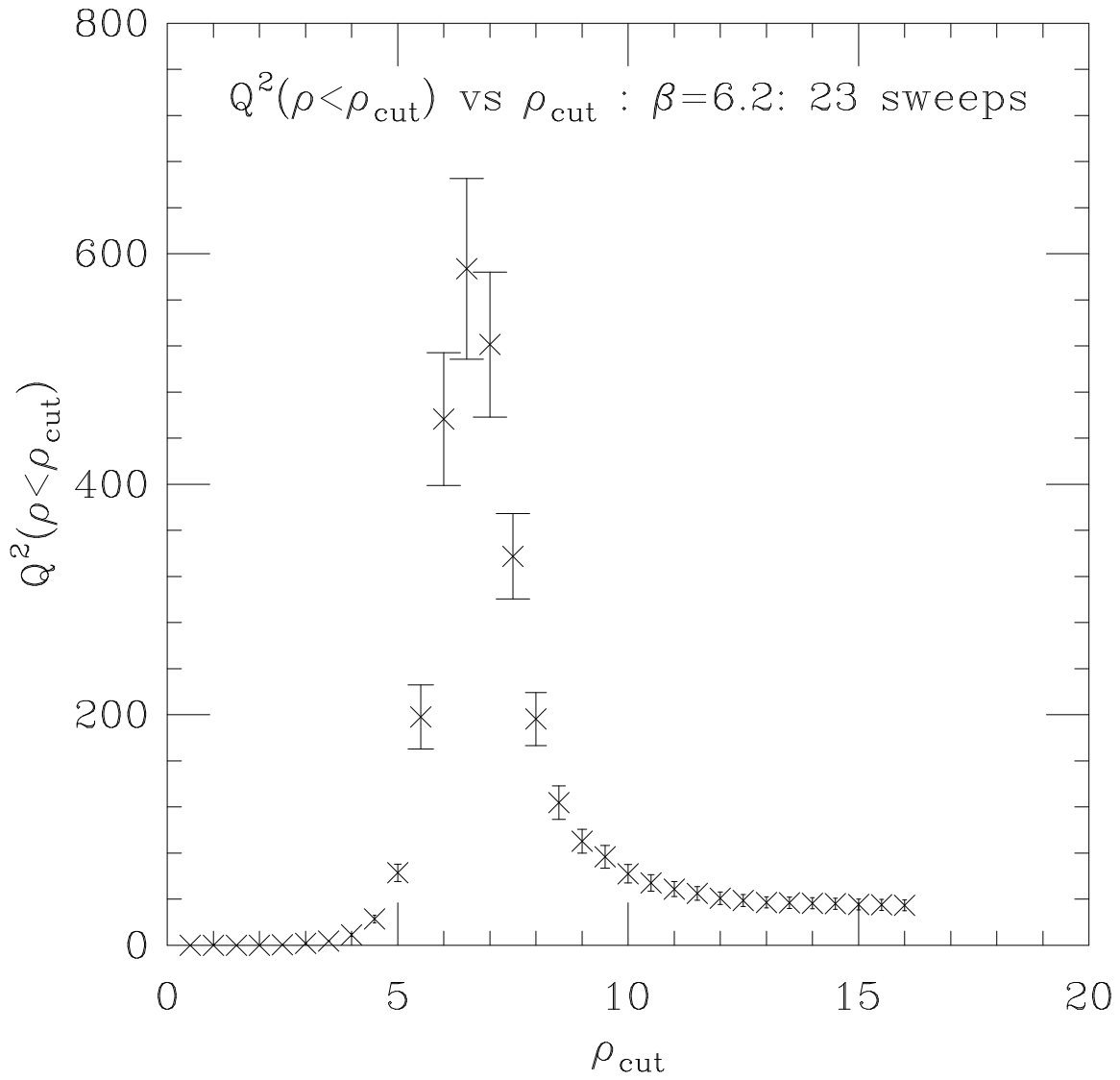


Figure 10: The average of  $Q^2$  when only charges with sizes  $\rho < \rho_c$  are included : at  $\beta = 6.2$  after 23 cooling sweeps

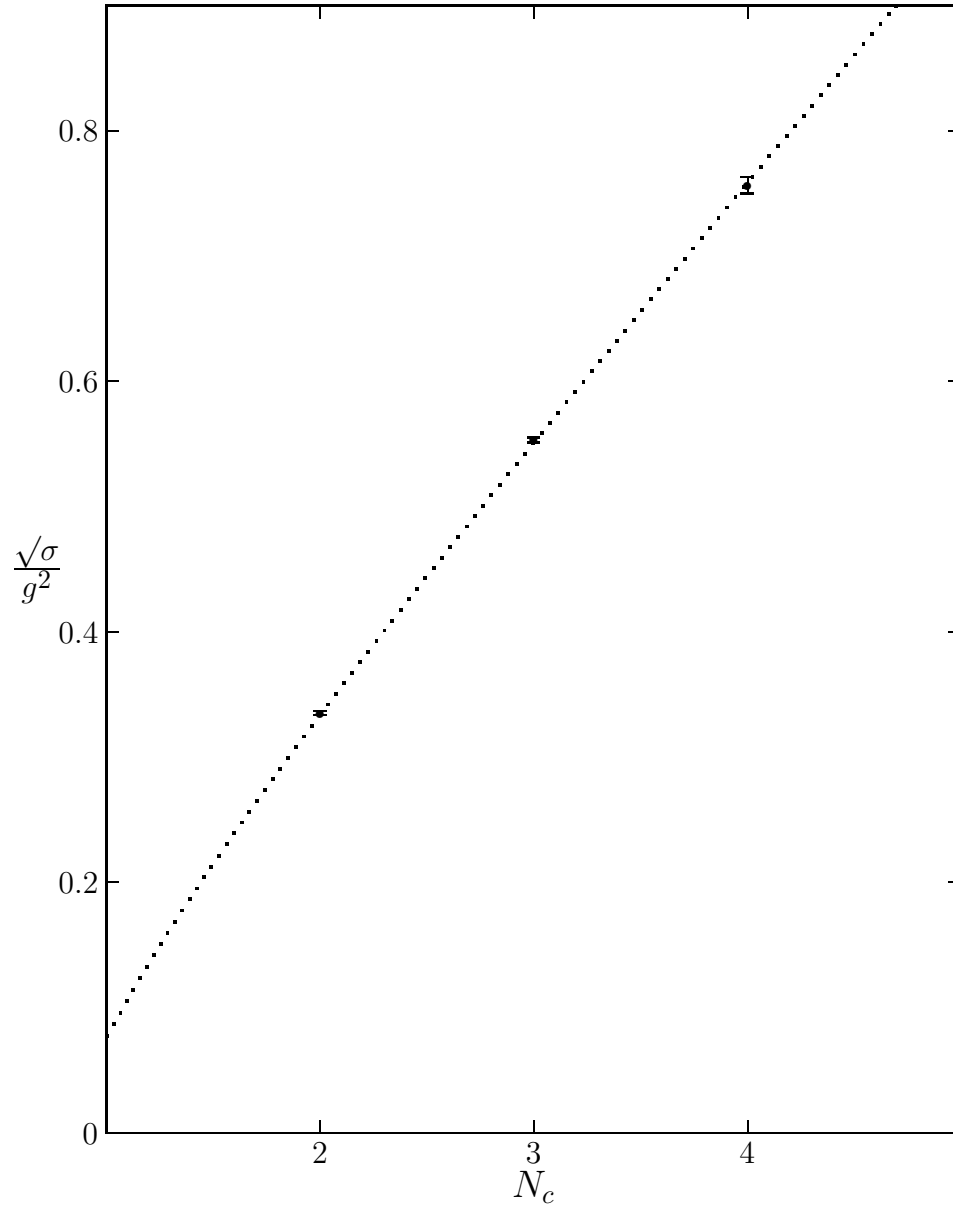


Figure 11: Continuum string tension versus number of colours in  $D = 2 + 1$ . Line is the fit in eqn 33.

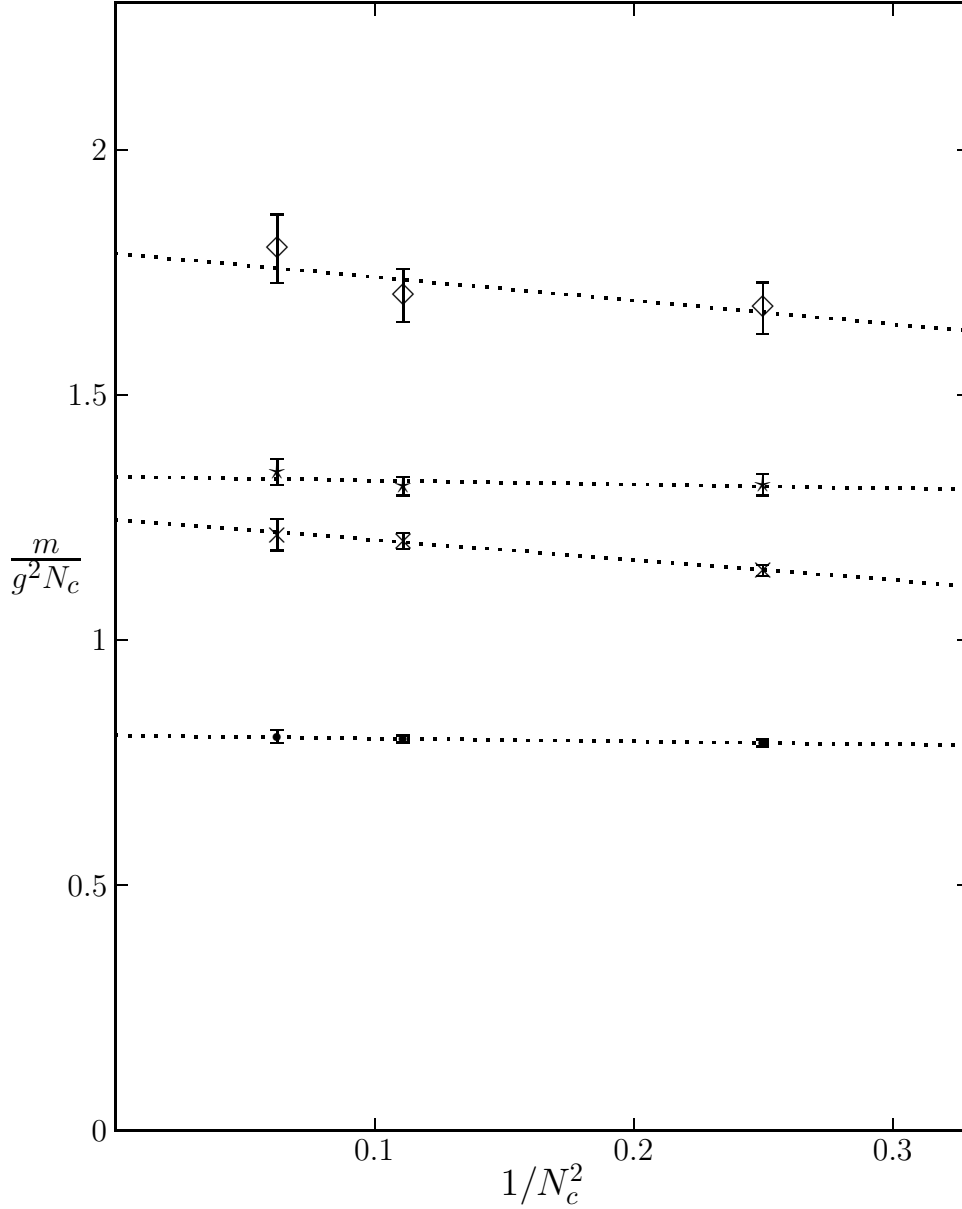


Figure 12: Some continuum glueball masses, in  $D = 3$ , for 2,3,4 colours:  $0^{++}$ ( $\bullet$ ),  $0^{++*}$ ( $\times$ ),  $2^{++}$ ( $\star$ ),  $0^{-+}$ ( $\diamond$ ) and linear fits.

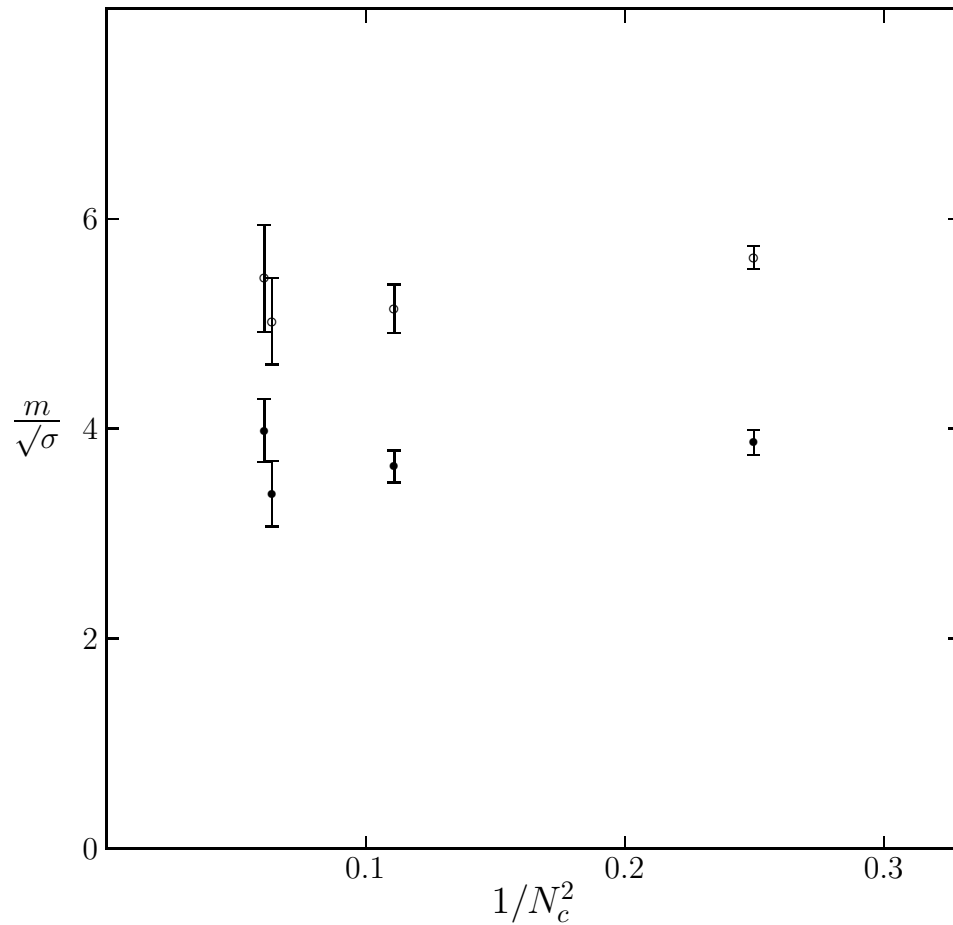


Figure 13: Lightest scalar ( $\bullet$ ) and tensor ( $\circ$ ) glueball masses in  $D = 4$ . Continuum values for  $N_c = 2, 3$  and lattice values ( $\beta = 10.9$  and  $\beta = 11.1$ ) for  $N_c = 4$ .

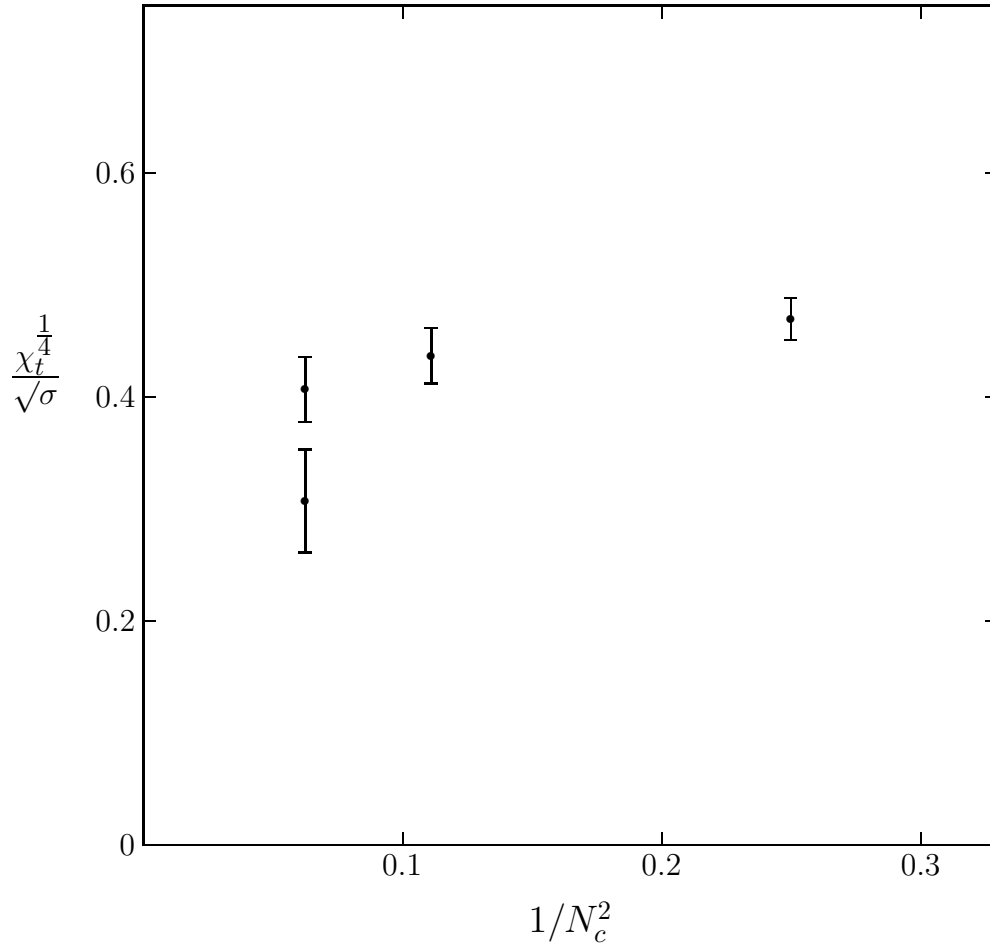


Figure 14: The topological susceptibility: continuum values for  $N_c = 2, 3$  and lattice values ( $\beta = 10.9$  and  $\beta = 11.1$ ) for  $N_c = 4$ .